HHS Public Access

Author manuscript

Anesthesiology. Author manuscript; available in PMC 2017 February 01.

Published in final edited form as:

Anesthesiology. 2016 February ; 124(2): 428–442. doi:10.1097/ALN.0000000000000974.

Insulin Signaling in Bupivacaine-induced Cardiac Toxicity: Sensitization during Recovery and Potentiation by Lipid Emulsion

Michael R. Fettiplace, MS[*,1,2,3], **Katarzyna Kowal, BS**[1,2], **Richard Ripper, CVT**[1,2], **Alexandria Young, BS**[1,2], **Kinga Lis, BS**[1,2], **Israel Rubinstein, MD**[2,4], **Marcelo Bonini, PhD**[4], **Richard Minshall, PhD**[1], and **Guy Weinberg, MD**[1,2]

[1]Department of Anesthesiology, University of Illinois College of Medicine, Chicago, Illinois

[2]Research & Development Service, Jesse Brown Veterans Affairs Medical Center, Chicago, IL

[3]Neuroscience Program, University of Illinois at Chicago, Chicago, IL

[4]Department of Medicine, University of Illinois College of Medicine, Chicago, IL, University of Illinois at Chicago, University of Illinois College of Medicine, Chicago, Illinois, USA

Abstract

Background—The impact of local anesthetics on regulation of glucose homeostasis by protein kinase B (Akt) and 5'-Adenosine monophosphate activated protein kinase (AMPK) is unclear but important because of the implications for both local anesthetic toxicity and its reversal by intravenous lipid emulsion (ILE).

Methods—Sprague-Dawley rats received 10mg/kg bupivacaine over 20 seconds followed by nothing or 10mL/kg ILE (or ILE without bupivacaine). At key time points, heart and kidney were excised. Glycogen content and phosphorylation levels of Akt, p70s6k, s6, IRS1, GSK-3β, AMPK, ACC, TSC2 were quantified. Three animals received Wortmannin to irreversibily inhibit phosphoinositide-3-kinase (Pi3k) signaling. Isolated heart studies were conducted with bupivacaine and LY294002—a reversible Pi3K inhibitor.

Results—Bupivacaine cardiotoxicity rapidly de-phosphorylated Akt at S473 to 63 ± 5% of baseline and phosphorylated AMPK to 151 ± 19%. AMPK activation inhibited targets downstream of mTORC1 via TSC2. Feedback dephosphorylation of IRS1 to 31 ± 8% of baseline sensitized Akt signaling in hearts resulting in hyper-phosphorylation of Akt at T308 and GSK-3β to 390 ± 64% and 293 ± 50% of baseline respectively. Glycogen accumulated to 142 ± 7% of baseline. Irreversible inhibition of Pi3k upstream of Akt exacerbated bupivacaine cardiotoxicity, while pretreating with a reversible inhibitor delayed onset of toxicity. ILE rapidly phosphorylated

Corresponding Author: Michael Fettiplace, MS, MD/Ph.D. candidate, Department of Anesthesiology (M/C515), University of Illinois Hospital & Health Sciences System, 1740 W Taylor, Chicago, IL 60612, Phone: 410-900-4498, Fax: 312-569-8114, mfetti3@uic.edu.

Conflicts of Interest: Dr. Weinberg was awarded a US patent related to lipid resuscitation, is co-founder of ResQ Pharma, Inc with Dr. Rubinstein and established the educational website, www.lipidrescue.org, an educational Web site on lipid emulsion as treatment of drug overdose and toxicity. The other authors declare no competing interests.

Akt at S473 and T308 to 150 ± 23% and 167 ± 10% of baseline, respectively but did not interfere with AMPK or targets of mTORC1.

Conclusion—Glucose handling by Akt and AMPK is integral to recovery from bupivacaine cardiotoxicity and modulation of these pathways by ILE contributes to lipid resuscitation.

Keywords

bupivacaine; local-anesthetic; lipid emulsion; AMPK; Akt; mTOR; IRS1

Introduction

Bupivacaine toxicity is an uncommon but life-threatening event [1,2]. If toxicity occurs in the clinical setting, an infusion of lipid emulsion (ILE) is used to accelerate recovery. The mechanism of ILE-based reversal of toxicity includes both a scavenging effect and a direct effect that improves cardiac output [3]. This improvement of cardiac output is seen in the absence of toxicity [4] and contributes to the rapid recovery from toxicity [5]. However the cellular signaling underlying this effect is unknown. Recent reports demonstrate that bupivacaine disrupts targets of classical insulin signaling [6] including protein kinase B (Akt) and ribosomal protein s6 kinase 1, in cellular models [7,8]. Further, the amide-linked local anesthetics, ropivacaine and lidocaine, disrupt assembly of phosphoinositide-3-kinase (Pi3k) thereby blocking phosphorylation of Akt [9], an effect that is independent of classical sodium-channel blockade [10]. Beyond Akt, bupivacaine activates other controllers of glucose homeostasis, including 5’ adenosine monophosphate activated protein kinase (AMPK) [11,12], an effect which may provide cyto-protection during toxicity [13]. Conversely, ILE and other fatty-acids increase phosphorylation of Akt and other canonical insulinergic targets when used as an adjuvant in recovery from ischemia-reperfusion injury [14–18]. In the absence of toxicity, lipid emulsions modulate AMPK in a number of different tissues [19]. Based on this evidence, we hypothesized that bupivacaine-induced cardiac-toxicity adversely affects cellular signaling at targets of glucose homeostasis, including Akt and AMPK [6], and that recovery with ILE modifies this process.

Methods

Rats were housed as pairs in the Veterinary Medical Unit at the Jesse Brown Veterans Affairs Medical Center (JBVAMC, Chicago, IL). Experiments were conducted under sterile conditions in the Veterinary Medical Unit at the JBVAMC. Protocols were approved by the Institutional Animal Care and Utilization Committee of the JBVAMC (IACUC protocol #12–18).

In vivo model

Sprague Dawley rats (n=29) weighing between 372–426g were induced with isoflurance in a bell jar before we performed a tracheotomy for intubation and maintained them on 1.2–1.75% isoflurane for the remainder of the experiment. Animals were instrumented with a carotid catheter to measure blood pressure, bilateral jugular catheters for infusions and three electrodes to measure electrocardiogram. Following a 30-minute equilibration period, animals received 10mg/kg bupivacaine hydrochloride into the left internal jugular over 20

seconds to produce a transient asystole. A subset of animals also received adjuvant ILE (10mg/kg, 30% Intralipid®, Baxter Pharmaceuticals, Deerfield IL). At pre-specified time-points (1.5, 5 & 10 minutes) following injection, animals were sacrificed by rapid cardiac excision. Tissue was immediately frozen in liquid nitrogen. The peritoneum was opened and the right kidney was removed and frozen in liquid nitrogen as well. Three animals were pretreated 10 minutes prior to bupivacaine with 25μg/kg of intravenous Wortmannin (Sigma-Aldrich, St. Louis MO). Additionally, a group of animals (n=8) received only 10mL/kg lipid emulsion (over 1 minute, with no bupivacaine) and were sacrificed at 3.5 minutes after infusion (matched to the 5-minute bupivacaine +ILE time-point). Tissues were prepared in a similar manner. Physiological data was recorded with LabChart 7.0 (ADInstruments, Colorado Springs, CO).

Ex Vivo Isolated Hearts

Sprague Dawley rats (n=20) were anesthetized by intraperitoneal injection of 60mg/kg sodium pentobarbital (Abbott Labs, Abbott Park, IL). Animals were heparinized prior to cardiac excision. Hearts were suspended from a Langendorff apparatus, cannulated at the aortic root, and perfused by roller pump at a rate of 16mL/min with Krebs-Henseleit buffer (100 mM NaCl, 4.74 mM KCl, 1.18 mMKH2PO4, 1.18 mM MgSO4, 1.00 mM CaCl2, 25.00 mM NaHCO3, 11.50mM glucose, 4.92mM pyruvate, 5.39mM fumarate), at 37°C and pH 7.40. The buffer was equilibrated with a mixture of oxygen (95%) and carbon dioxide (5%) by passing through a membrane oxygenator. Pressure was transduced from a latex balloon in the left ventricle and recorded using Chart 7.0. Drugs were delivered by syringe pump to stopcocks ~2cm above the aortic valve. Fourteen hearts were randomized to receive nothing (n=2), 500 μM bupivacaine over 30 seconds (n=6) or 500 μM bupivacaine over 30 seconds with pretreatment of 50μM LY294002 (Sigma-Aldrich, St Louis, MO) over 1 minute (n=6). Two minutes after completion of infusion, hearts were flash frozen in order to ensure cardiac bupivacaine concentrations were in accordance with previous experiments [20]. The remaining six hearts received 20% ILE (10mg/kg 20% Intralipid®) over ten minutes infused to a 1% final concentration. Samples of left ventricle were harvested immediately prior to infusion and at 10-minutes and flash-frozen in liquid nitrogen.

Western Blotting

All procedures were conducted on ice. The apex of heart and apical pole (cortex only) of the left kidney were isolated. Approximately 100mg of tissue was dissected, washed and homogenized in 1.5mL lysis buffer using an Omni Mixer Homogenizer (Omni International, Kennasaw GA). Lysis buffer comprised 18mM Tris-HCl, 114mM NaCl, 0.4% sodium deoxycholate, 0.1% Sodium Dodecyl Sulfate, 9mM sodium pyrophosphate, 0.9mM sodium Fluoride, 9% glycerol, 10% Triton X-100, 10mM sodium orthovanadate, 1mM phenylmethanesulfonyl fluoride, 1mM Dithiothreitol with pH adjusted to 7.4 and supplemented with Roche Complete Mini EDTA-free tablet (Roche Diagnostic Corporation, Indianapolis, IN). Samples were spun at 14K rpm for 10 minutes to remove insoluble tissue and membranes. Total protein concentration was quantified using a Pierce BCA Protein assay (Thermo Scientific, Rockford, IL) and iMark microabsorbance plate reader (BioRad, Hercules CA). Samples were aliquoted into 50mL portions and refrozen at −80°C. 20μg of protein were loaded and run on a 4–15% miniPROTEAN® TGX gel (BioRad, Hercules,

CA), then transferred to nitrocellulose membrane (ThermoScientific, Rockford, IL). Membranes were blotted for 30 minutes with 5% bovine serum albumin Cohn fraction V (Sigma Aldrich), washed and incubated with rabbit anti-mouse primary antibodies against pT308 Akt, pS473 Akt, total Akt, pT172 AMPK, pS79 acetyl CoA carboxylase (ACC), pS21/pS9 glycogen synthase kinase 3 α/β, pT421 p70 s6 kinase (p70s6k), pS235 ribosomal protein s6, pS1387 tuberous sclerosis 2 (TSC2), pS612 insulin receptor substrate 1 (IRS1) and total glyceraldehyde 3-phosphate dehydrogenase (GAPDH) as loading control (all antibodies from Cell Signaling Technologies, Waltham, MA). Subsequently, membranes were washed and incubated with goat anti-rabbit IgG linked to horseradish peroxidase-peroxidase (Cell Signaling). Luminescence was induced with Amersham ECL Prime (GE Biosystems) and exposed under dark-room conditions on care-stream autoradiography film (Sigma-Aldrich, St. Louis MO). Protein quantification was conducted in ImageJ (National Institutes of Health, Bethesda, MD). To control for equal loading, samples were quantified and normalized to total GAPDH. For AMPK and Akt, phospho-protein level was subsequently normalized to total protein level. Since time-points were early, we did not anticipate major protein synthesis or degradation, and since no changes were observed in total AMPK and Akt, we did not measure (or normalize) total protein levels for other phospho-proteins.

Glycogen Quantification

Glycogen levels were measured with a colorimetric assay (MAK016, Sigma Aldrich, St Louis, MO). Left ventricular tissue was isolated, homogenized and lysed. Lysate was spun and supernatant transferred into tubes for quantification. Glycogen was degraded to glucose with hydrolysis enzyme mix and developed with a colorimetric development enzyme mix. Subsequent coloration coupled to the amount of glycogen in the sample was quantified using an iMark microabsorbance plate reader (BioRad, Hercules, CA).

Bupivacaine concentration fit curves & grouping

Fit curves for bupivacaine concentrations in heart and kidney were developed based on data in Fettiplace et al, 2015 [3]. In brief, concentration of drug in tissue was plotted against time and fit to a single-phase exponential decay with a y-intercept held at zero. As described in the prior publication, recovery of cardiovascular parameters (carotid flow and blood pressure) is coincident with cardiac bupivacaine concentrations dropping below known inhibitory concentrations for voltage-gated ion channels. In those experiments, carotid flow was depressed when cardiac bupivacaine concentrations were >100 nmol/g but flows recovered below 100nmol/g and peaked ~50nmol/g. This provided a grouping mechanic based on a “recovery threshold” that reflects recovery of cardiovascular parameters and myocardial drug-concentrations either above or below ~100nmol/g. This level is consistent with the half-maximal inhibitory concentration (IC_{50}) of bupivacaine for cardiac sodium channels and cardiac calcium channels. Based on data from prior publications[3,21–23], the IC_{50} for sodium and calcium channels translate to tissues concentrations of 87μM and 80μM respectively for both cardiac and kidney tissue. The >100μM group includes animals sampled at 1.5 & 5 minutes and the <100μM group includes animals at the 10 minutes time-point. Animals receiving ILE in the <100μM+ILE group were sampled at the 5-minute time

point. Kidney was used as a control for contractile status. Recovery was ignored and groups were analyzed based on kidney bupivacaine concentrations >100μM.

Statistical Analysis and Power quantification

Omnibus testing was conducted by 2-way ANOVA with matched samples grouped by kinase and time-point. Post-hoc differences were assessed by Sidak tests to control for multiple-comparisons. Groupwise alpha was set at 0.05. Since data were non-normal with large differences in scale and variance, data were ranked prior to statistical testing to provide normalization [24,25]. Physiological and recovery parameters without grouping components were assessed with double-sided Mann-Whitney U-tests. A pilot set of animals in the bupivacaine only group (control, 1, 5, 10 minute), bupivacaine + ILE group (1, 5 10 minutes), and lipid only group at 5 minutes were run to make power calculations. For comparisons against baseline we determined a sample size of 8 (4 per group) based on a Cohen's d of 2.8, power=0.8 and alpha=0.05 for bupivacaine comparisons. For the bupivacaine+ILE and ILE alone we expected a robust effect size but anticipated the need for a larger sample size (10) based on a slightly smaller Cohen's d (~2.3) due to larger variance of values during recovery. Physiological data and densitometry data are expressed as mean ± SEM.

Results

I. Bupivacaine toxicity inhibits Akt & targets downstream of mTORC1 signaling in cardiac tissue

We used a previously characterized single intravenous injection model of low-dose bupivacaine toxicity[3,5,26] to assess kinase phosphorylation and dephosphorylation in cardiac tissue in response to a recoverable dose of bupivacaine. The advantage of this model is that after rapid onset of asystole, animals recover without further intervention (Figure 1A). The gradual improvement in cardiac output is coincident with cardiac bupivacaine content falling below the IC_{50} for multiple voltage-gated ion channels in the heart (Figure 1B) providing a grouping mechanism based on recovery status and tissue concentration of bupivacaine that reflects level of channel inhibition (see Methods: Bupivacaine concentration fit curves & grouping). Unrecovered (e.g. cardiac bupivacaine >100μM) animals from the 1.5 minutes & 5-minute time-points were anticipated to have cardiac bupivacaine concentrations of 301 ± 23 (95%CI) and 152 ± 25 nmol/g (95%CI) respectively. Recovered animals (e.g. cardiac bupivacaine <100μM) from the 10-minute post-challenge time point were expected to have cardiac bupivacaine concentration of 57 ± 21nmol/g (95%CI). At the ten minute time point when cardiac bupivacaine was <100μM, rate-pressure-product (RPP) had improved to 37 ± 2% of baseline (mean ± SEM) as compared with 15 ± 6% at the 1.5 and 5 minute time-points (p=0.01, Figure 1C).

We examined changes in cellular signaling by western blotting for phospho-proteins in the insulinergic pathway. We quantified concentrations of Akt phosphorylated at S473 & T308, and the downstream targets GSK-3β at S9, p70s6k at T421, ribosomal protein s6 at S235, and feedback phosphorylation of IRS1 at S612 (Figure 1D). Consistent with previous reports [7–9], bupivacaine reduced signaling in the Akt pathway with treatment accounting for

48% of the effect (Figure 1E, 2-way matched sample ANOVA interaction p=0.0035, kinase effect p=0.0035, treatment effect p=0.0083, matching p<0.0001). Phosphorylation was decreased on Akt at S473 to 63 ± 5% (mean ± SEM, Sidak post-test p=0.017), p70s6k at T421 to 50 ± 17% (p=0.0043), ribosomal protein s6 at S235 to 44 ± 11% (p=0.0015) and IRS1 at S612 to 31 ± 8% (p=0.0004) compared to baseline values. However targets directly downstream of Pi3k (T308 on Akt and S9 on GSK-3β) were less consistently affected with reductions on Akt at T308 to 85 ± 25% of baseline (p=0.98; 95% confidence interval: 0.23–1.33) and GSK-3β at S9 to 75 ± 17% of baseline (p=0.42; 95% confidence interval: 0.27–1.06).

II. Bupivacaine toxicity activates AMPK in cardiac tissue

In order to resolve the discrepancy that targets downstream of the mammalian target of rapamycin complex 1 (mTORC1) including p70s6k & s6 were preferentially affected, we looked to test other signaling targets. Specifically, 5'-adenosine-monophosphate kinase (AMPK) provides a countervailing force at tuberous sclerosis 2 (TSC2) that inhibits mTORC1 and downstream targets (Figure 2A) and has been implicated in cellular models of bupivacaine toxicity [11,12]. We probed for phosphorylation of AMPK at T172 and its downstream targets, Acetyl CoA Carboxylase (ACC) at S79 and TSC2 at S1387 (Figure 2B). We again found that treatment accounted for the largest portion of the variation (77%) in group-wise comparison (2-way matched sample ANOVA: interaction p<0.0001, kinase effect p<0.0001, treatment effect p<0.0011, matching p<0.0001). Across all time-points, phosphorylation increased to 151 ± 19% of baseline at T172 on AMPK (Sidak: p=0.0001), 179 ± 32% of baseline at S79 on ACC (p=0.0001, Figure 2C), and 1266 ± 258% of baseline at S1387 on TSC2 (p=0.0001, Figure 2D).

III. Activation of insulinergic signaling during recovery

We next analyzed the phosphorylation status (of this pathway) during recovery. We found that at the 10-minute time-point (when cardiac bupivacaine concentrations were <100μM), there was a marked increase in phosphorylation of key signaling proteins above baseline levels (e.g. hyper-phosphorylation). This hyper-phosphorylation was observed in Akt at S473 to 378± 84% of baseline (Sidak: p<0.0001) & T308 to 390 ± 64% of baseline (p<0.0001), GSK3β at S9 to 293 ± 50% of baseline (p=0.0005), p70s6k at T421 to 203 ± 29% of baseline (p=0.0002) and IRS1 at S612 to 186 ± 37% of baseline (p<0.0001, Figure 3A) in comparison to unrecovered animals (2-way matched subject ANOVA: interaction p<0.0001, kinase effect p<0.0001, recovery effect p=0.002, matching p<0.0001). We further assessed for biochemical changes by examining cardiac glycogen content in these hearts and found an increase in glycogen from 2.4 ± 0.17 μm/g to 3.4 ± 0.26 μm/g (Mann-Whitney U-test p=0.006, Figure 3B). Both of these changes are consistent with a sensitization to canonical insulin signaling caused by the loss of negative feedback to IRS1 (Figure 3C).

IV. Akt signaling is blunted in Kidney

In order to confirm that the loss of phosphorylation following bupivacaine challenge was not a contractile or flow-dependent phenomenon, we assayed for phosphorylation changes in the kidney which experiences very high bupivacaine concentrations in this experimental system (Figure 4A) but is not subject to contractile effects. We assessed phosphorylation of Akt at

S473 and T308 as well as phosphorylation of the downstream target GSK3β at S9 (Figure 4B, Figure 4C) at three time points when bupivacaine concentrations were above channel blocking thresholds with an expected concentration of 171 ± 25nmol/g (95% CI). There was a marked treatment-specific effect (2-way ANOVA, treatment $p<0.0001$ 69% of variation) with no interaction ($p=0.93$) or kinase ($p=0.93$) effect. There was a decrease in Akt phosphorylation at S473 to 56 ± 13% of baseline ($n=8$, $p=0.0015$, Sidak post-test), a decrease in Akt phosphorylation at T308 to 62 ± 11% of baseline ($n=5$, $p=0.0012$, Sidak post-test), and a decrease in GSK-3β phosphorylation at S9 to 42 ± 18% of baseline ($n=5$, $p=0.0041$, Sidak post-test).

V. Blocking pi3k signaling exacerbates recovery

We used pharmacological inhibitors to assess whether interfering with this pathway modifies recovery. In the in vivo system, we used the irreversible Pi3k inhibitor—Wortmannin (Figure 5A)—to determine if sensitization to insulin signaling and subsequent activation of Akt is required for recovery. Animals were pretreated with Wortmannin and 10 minutes later subjected to the standard bupivacaine infusion, sacrificed at 10-minutes and phosphorylation of targets downstream from Pi3k were assessed (Figure 5B). Treatment with Wortmannin raised blood pressures by ~20mmHg in one animal but did not have any other prominent effects. Consistent with the effect of Wortmannin we found that phosphorylation of proteins was reduced in comparison to the animals that were not treated with Wortmannin (Figure 5C, 2-way matched sample ANOVA, treatment effect 74% of variation, $p=0.0011$, kinase effect $p<0.0001$, interaction $p=0.0003$, matching $p<0.0001$). In addition, Wortmannin blunted recovery from toxicity, reducing cardiac output at 10-minutes to 12 ± 8% of baseline in contrast to 37 ± 2% of baseline in the animals not treated with Wortmannin ($p=0.03$) (Figure 5D). In order to ensure that this was a cardiac specific effect we tested the effect of the specific pi3k inhibitor LY294002 on bupivacaine toxicity in an isolated heart system with a constant flow state. Animals were acutely treated with LY294002 1 minute prior to bupivacaine toxicity and then subjected to a bupivacaine challenge. Time to recovery was not different between groups (Figure 5E), and physiological parameters were not different upon recovery (Figure 5F) but pretreatment with LY294002 significantly delayed the time until occurrence of asystole, with three animals in the LY group not experiencing asystole until after the bupivacaine infusion was stopped (Figure 5G).

VI. Lipid emulsion accelerates physiological recovery

Next, we characterized the effect of ILE supplementation on kinase phosphorylation during recovery. Consistent with previous reports[5], treatment with ILE accelerated physiological recovery from toxicity (Figure 6A) and by five minutes animals treated with ILE had achieved 98 ± 7% of baseline RPP compared with untreated animals who were at 18 ± 9% of baseline (Mann-Whitney U-test, $p=0.002$). While animals in the control group began to recover by ten minutes, their cardiac function remained depressed compared to that of the ILE group (37 ± 2% versus 80 ± 13% compared to baseline RPP for control and ILE respectively; $p=0.005$). As with the untreated group, this recovery was coincident with a time point when cardiac bupivacaine concentrations fell below the IC_{50} for cardiac sodium

channels (Figure 6B). For animals receiving ILE in the <100μM+ILE group, the expected cardiac bupivacaine concentration is 59 ± 23nmol/g (95%CI).

VII. Lipid emulsion drives time-dependent phosphorylation of Akt during toxicity but not proteins downstream of mTORC1

Next we assessed phosphorylation of proteins in the insulinergic pathway including pT308-Akt, pS473-Akt, pS9-GSK3β, pT421 p70s6k, pS235 ribosomal protein s6, and pS612 IRS1 at predetermined time-points (1.5, 5, & 10 minutes) during recovery following ILE treatment (Figure 7A). Consistent with observations during spontaneous recovery from bupivacaine toxicity, we observed hyper-phosphorylation in the pathway at the 10-minute time-point for all proteins (not pictured). However, following ILE at the 5-minute time-point when cardiovascular parameters are recovered and cardiac bupivacaine concentration is below the IC_{50} for cardiac sodium channels (Figure 6A & B) we found significant differences from baseline values for phosphorylation of key proteins (Figure 7B, 2-way ANOVA, treatment effect p=0.004, kinase effect p<0.0001, interaction p<0.0001). Akt was phosphorylated at both S473 (Sidak: p=0.0026) to 150 ± 23 % of baseline and at T308 (p=0.0004) to 167 ± 10 % of baseline. No change in phosphorylation was seen in s9-GSK-3β (98 ± 14 of baseline). Downstream of mTORC1 we observed de-phosphorylation of p70, s6 and loss of feedback phosphorylation of IRS1: pT421 p70s6k was reduced to 41 ± 16%, p=0.0005; S235 ribosomal protein s6 reduced to 52 ±14%, p=0.0002, and feedback phosphorylation of S612-IRS1 was reduced to 45 ±12%, p<0.0001; compared to baseline. We confirmed these effects by regressing the data-points across time. For the predominant insulinergic phosphorylation site on Akt (T308) there was a positive linear regression against time as relative phosphorylation levels of T308 fit to a linear slope (R=0.85) with a non-zero slope of 16 ± 3 %*min^{-1} (p<0.0001, Figure 7C), and a y-intercept of 100 ± 2%. Downstream of mTORC1, relative phosphorylation levels on threonine 421 of p70s6k also fit to a linear slope (R = 0.89) of 28 ± 6 %*min^{-1} (p>0.0001) but with a y-intercept of 55 ± 4% that did not include 100% (Figure 7D).

VIII. Phosphorylation of TSC2 downstream of AMPK remains consistent through toxicity despite lipid emulsion treatment

In order to assess the source of discordance upstream and downstream of mTORC1, we measured phosphorylation levels of AMPK, ACC (Figure 8A) and TSC2 (Figure 8B), in the presence of adjuvant ILE. Consistent with the untreated condition, treatment with the combination of bupivacaine and ILE leads to a robust treatment-specific effect on phosphorylation (2-way ANOVA, p=0.0002) but no kinase or interaction effects. AMPK was phosphorylated at T172 to 145 ± 20% of baseline (p=0.1125) and TSC2 was phosphorylated at S1387 to 170 ± 11 % of baseline (p=0.0033); notably, the latter value was similar to that in the context of bupivacaine alone (Figure 8C).

X. Lipid emulsion drives phosphorylation of Akt in the absence of toxicity

Finally, we measured the ability of ILE to change phosphorylation levels of signaling proteins in the absence of toxicity (Figure 9A). For this, we injected animals with ILE (with no accompanying bupivacaine) and sacrificed at a time-point matched to the 5-minute bupivacaine & ILE time-point. At this matched time-point ILE produced a robust treatment

effect (2-way ANOVA: $p<0.0001$) without kinase or interaction effects. We found that ILE rapidly increased phosphorylation of Akt at both T308 (Sidak: $p=0.0192$) and S473 ($p=0.0192$, Figure 9B). Further, there was feedback phosphorylation of IRS1 at S612 ($p=0.0229$), a phenomenon that is known to contribute to insulin resistance in peripheral skeletal muscle [27–29]. There were no lipid-induced changes in phosphorylation at downstream targets including GSK-3β, p70s6k or s6. We also found that treatment with ILE alone contributed to glycogen accumulation in the heart (Figure 9C). Next we checked the effect of ILE on AMPK, ACC and TSC2 phosphorylation to determine whether activation of AMPK resulted from ILE or bupivacaine treatment (Figure 9D). Treatment with ILE in the absence of toxicity had no appreciable effects on phosphorylation of AMPK, ACC or TSC2 (Figure 9E, 2-way matched subjects ANOVA, treatment $p=0.35$, kinase $p=0.0978$, interaction $p=0.0978$).

Discussion

We found in a rat model that systemic bupivacaine toxicity is a dynamic insult whereby fundamentally distinct and separate effects on insulinergic signaling (i.e. pi3k, Akt, IRS1, etc) and glucose homeostasis (i.e. AMPK, GSK-3β) occur during induction of toxicity and recovery from it. Our results agree with previous in vitro studies wherein lethal or cytotoxic concentrations of bupivacaine induce de-phosphorylation of Akt [7–9] and phosphorylation of AMPK [11,12]. Both of these kinases integrate signaling at mTORC1 to modulate sensitivity to endogenous insulin[30] during recovery from toxicity. As such, we also found that bupivacaine toxicity reduced signaling downstream of Raptor & TSC2 (Figure 10A). The loss of signaling from p70s6k to IRS1 sensitizes insulinergic pathways. Consistent with this, we observed that recovery from bupivacaine-induced cardiac toxicity was associated with hyper-activation of insulinergic targets and a ~40% increase in cardiac glycogen stores (Figure 10B), which is associated with better outcomes from cardiac ischemia[31]. Modulation of glycogen levels by AMPK is asserted to protect against post-ischemic dysfunction[32]. The sensitization of signaling serves as a protective mechanism to normalize energy processing in settings where metabolism is impaired. Blocking sensitization with Wortmannin, an irreversible inhibitor of Pi3k, interfered with recovery. Transiently blocking Pi3k with the reversible inhibitor—LY20794—provided resistance to toxicity. These findings implicate the importance of this pathway and associated kinases in response to drug toxicity. Wortmannin can also interfere with mTORC1 signaling so the importance of the AMPK pathway is reinforced by the findings.

Adjuvant lipid emulsion drives Akt

We found that ILE produced rapid changes to insulinergic signaling at Akt and other targets co-incident with recovery from toxicity. Treatment with ILE in the absence of bupivacaine toxicity activated insulin signaling at Akt but had no effect on AMPK (Figure 11A). In combination, bupivacaine and ILE provided concurrent activation of both AMPK and Akt. AMPK blocked mTORC1 & downstream targets (p70,s6,IRS1) while the addition of ILE induced early re-phosphorylation of Akt, upstream of mTORC1 (Figure 11B). One of our more interesting findings was the rapidity with which these systems turned on and off. AMPK, Akt and downstream targets were significantly altered at our earliest time-point (1.5

minutes) and again by 10-minutes, when Akt was fully re-phosphorylated. Lipid emulsion drives rapid physiological changes both in the context of toxicity and in its absence that could be mediated by changes in signaling [4,33]. The involvement of these pathways also points to other treatments for toxicity that could accelerate recovery through modulation of metabolic or signaling pathways.

Local anesthetics and Insulin signaling

Local anesthetics are known to modulate energy processing as carnitine deficiency sensitizes animals to bupivacaine toxicity[34], a finding that confirmed the clinical observation that carnitine deficiency predisposes patients to bupivacaine toxicity[35,36]. Further, local-anesthetics inhibit mitochondrial carnitine exchange in experimental models [37,38] and supplementation of ATP can overcome bupivacaine toxicity in myocardial cells [39]. Beyond energy production, a number of clinical and experimental observations comport with the conclusion that local anesthetics modify insulin signaling. Hypoglycemic or streptozotocin-induced diabetic animals are more sensitive to bupivacaine cardiac toxicity [40,41] and insulin provides inotropic support during bupivacaine cardiac-toxicity [42,43]. In non-toxic situations, diabetic rats experience extended block durations independent of neurotoxicity [44–47] and patients with poorly-controlled diabetes experience extended duration of local-anesthetic induced peripheral nerve blocks [48–50] ; Despite the importance of understanding the interaction of local-anesthetic effects on diabetic patients [51], the connection between sensitization to toxicity and glucose handling has previously been incompletely addressed.

Conceivably, improvement in insulin signaling could increase myocardial contractility as both GSK-3β and Akt interact with contractile proteins downstream [52–55]. Multiple experimental models have demonstrated that bupivacaine can reduce infarct size in an ischemia-reperfusion model [56,57]. However, this effect is counterintuitive based on the research demonstrating that bupivacaine and similar amide-linked local anesthetics interfere with anti-apoptotic signaling by blocking Akt and downstream targets [7–9]. A sensitization to insulin signaling during recovery would provide a rational explanation for this effect. As an interesting aside, a clinical trial found that ILE unexpectedly reduced blood glucose levels when used as a treatment for xenobiotic drug overdose [58]. This finding comports with our observed connections between bupivacaine toxicity, lipid and insulin signaling.

Exacerbation of bupivacaine toxicity

A modification of glucose handling and sensitization of insulinergic signaling provides a new perspective on the mechanisms underlying physiological recovery from bupivacaine toxicity. Our results demonstrated that Wortmannin exacerbated bupivacaine cardiac toxicity. We know from previous studies that high-dose epinephrine, the classic PKA activator, can also interfere with recovery from bupivacaine toxicity [59]. Further, local-anesthetic toxicity produces an ischemic-like insult because of mitochondrial uncoupling [37,60]. It is conceivable that other drugs that exacerbate ischemia-reperfusion injury (opioid-receptor-antagonists, toll-like-receptor 2 antagonists, K_{ATP} channel antagonists, bradykinin antagonists, PKC inhibitors, etc) would make bupivacaine toxicity worse. Thus, appropriate controls are needed when studying lipid resuscitation therapy to differentiate worsening of toxicity from inhibition of the beneficial effects of ILE.

Clinical implications

From a clinical perspective, insulin has been used in the toxicology community for a number of years as a treatment for drug-induced cardiac toxicity. High-dose-insulin provides benefit in experimental models of bupivacaine toxicity [42,43] and is used in emergency rooms for other drug overdoses [61]. In particular calcium channel blocker (CCB) overdose is associated with a functionally hypo-insulinemic state (due to inhibition of insulin secretion) with secondary hyperglycemia. This allows physicians to follow blood glucose as a measure of both the severity of toxicity [62] and patient recovery [63]. Therefore, clinicians can predict recovery from CCB toxicity by observing dropping blood glucose levels, even before cardiovascular recovery. Experimentally, CCB's cause derangements in Pi3k signaling [64,65], a point in common with bupivacaine. Toxicity from tricyclic antidepressants also causes hyperglycemia [66], and treatment is associated with increased insulin sensitivity [67]. Following on this, high-dose-insulin therapy is potentially useful for tricyclic toxicity [61,68].

Lipid emulsion infusion has complex effects on metabolism, driving insulin resistance via diacyl-glycerol, protein kinase C and phosphorylation of IRS1 [27,28]. Further, it is known that fatty acids have a rapid uptake phase which accelerates the cycling of intracellular triacylglycerol stores [69] and this driving force is chain-length specific and exerts chain-length specific modification on cardiac contractility [70]. Beyond these basic concepts, the world of lipids in metabolism, signaling and disease is growing increasingly complex [71]. However, the acute effects of ILE are less well understood. If ILE can effectively modify insulin-signaling pathways to counter-act detrimental effects of drugs other than local anesthetics, then we may have a better heuristic to decide which drug overdoses are treatable with ILE. In particular, ILE provides benefit in CCB overdose [72–74] and tricyclic overdose [75,76] but the effect is less clear in beta-blocker overdose [77]. This comports with the aforementioned effects that CCBs and tricyclics have on blood sugar and insulin sensitivity.

Limitations

Our model lacked cardiac compressions, so that rats experienced hypoperfusion and tissue ischemia prior to hemodynamic recovery. Given that bupivacaine also produces an ischemia-like insult due to mitochondrial uncoupling, our results might reflect changes in Akt and AMPK secondary to ischemia, ATP depletion and glycolytic switching and not simply bupivacaine toxicity. If this is the case, then results from studies where ILE is used as an adjuvant for I/R injury[14–17] could be cross-applied to ischemic situations due to local anesthetic toxicity. As noted earlier, this would mean that treatments that adversely impact I/R injury could also worsen recovery from bupivacaine toxicity. Additionally, we did not probe all pathways involved in IRS1 sensitization. Both protein kinase C (PKC) and mitogen activated protein kinase (MAPK) pathways modulate IRS1 and might do so in the context of bupivacaine toxicity. Furthermore the inhibitors we used could modify binding of bupivacaine or change entry of drug across the plasma membrane.

Conclusion

Bupivacaine-induced cardiac toxicity activates AMPK and inhibits Akt with integration at TSC2 and loss of feedback from p70s6k to IRS1. This sensitizes cardiac tissue to

insulinergic signaling during recovery leading to hyper-activation of both Akt and GSK3β and the accumulation of glycogen as cardiac function improves. Preventing hyper-activation with Wortmannin—an irreversible pi3k inhibitor—exacerbates toxicity and demonstrates the importance of this pathway to recovery. In the absence of toxicity ILE drives phosphorylation of Akt upstream of mTORC1 but has no effect on the AMPK pathway. During toxicity, ILE also causes an early phosphorylation of Akt without perturbing the activation of AMPK by bupivacaine. As such, AMPK may be the primary actor in regard to toxicity while Akt may be more involved with recovery. If we use other methods to leverage these protective pathways (i.e. insulinergic sensitization, AMPK activation & Akt activation) we may be able to optimize treatment for bupivacaine and other drug overdose. Whether similar processes are also operating during other intentional and accidental drug overdose and poisoning merits further research.

Acknowledgments

Funding: M.R. Fettiplace was supported by an American Heart Association (Dallas, TX, USA) Predoctoral Fellowship 13PRE16810063 and the Department of Anesthesiology at the University of Illinois Hospital and Health Science Center. Guy Weinberg and Israel Rubinstein were funded by a United States Veterans Administration (Washington DC, USA) Merit Review and NIH CounterACT grant 1U01NS083457-01

References

1. Barrington MJ, Kluger R. Ultrasound guidance reduces the risk of local anesthetic systemic toxicity following peripheral nerve blockade. Reg Anesth Pain Med. 2013; 38:289–297. [PubMed: 23788067]
2. Albright G. Cardiac Arrest Following Regional Anesthesia with Etidocaine or Bupivacaine. Anesthesiology. 1979; 51:285–287. [PubMed: 484889]
3. Fettiplace MR, Lis K, Ripper R, Kowal K, Pichurko A, Vitello D, Rubinstein I, Schwartz D, Akpa BS, Weinberg G. Multi-modal contributions to detoxification of acute pharmacotoxicity by a triglyceride micro-emulsion. J Control Release. 2015; 198:62–70. [PubMed: 25483426]
4. Fettiplace MR, Ripper R, Lis K, Lin B, Lang J, Zider B, Wang J, Rubinstein I, Weinberg G. Rapid Cardiotonic Effects of Lipid Emulsion Infusion. Crit Care Med. 2013; 41:156–162.
5. Fettiplace MR, Akpa B, Ripper R, Zider B, Lang J, Rubinstein I, Weinberg G. Resuscitation with Lipid Emulsion : Dose-dependent Recovery from Cardiac Pharmacotoxicity Requires a Cardiotonic Effect. Anesthesiology. 2014; 120:915–925. [PubMed: 24496123]
6. Schultze SM, Hemmings Ba, Niessen M, Tschopp O. PI3K/AKT MAPK, AMPK signalling: protein kinases in glucose homeostasis. Expert Rev. Mol. Med. 2012; 14:1–21.
7. Maurice JM, Gan Y, Ma F, Chang Y, Hibner M, Huang Y. Bupivacaine causes cytotoxicity in mouse C2C12 myoblast cells: involvement of ERK and Akt signaling pathways. Acta pharmacol Sin. 2010; 31:493–500. [PubMed: 20228829]
8. Beigh MA, Showkat M, Bashir B, Bashir A, Hussain MU, Andrabi KI. Growth inhibition by bupivacaine is associated with inactivation of ribosomal protein s6 kinase 1. Biomed Res. Int. 2014; 2014:831845. [PubMed: 24605337]
9. Piegeler T, Votta-Vellis G, Bakhshi FR, Mao M, Carnegie G, Bonini MG, Schwartz DE, Borgeat A, Beck-Schimmer B, Minshall RD. Endothelial Barrier Protection by Local Anesthetics: Ropivacaine and Lidocaine Block Tumor Necrosis Tactor-α-Induced Endothelial Cell Src Activation. Anesthesiology. 2014; 120:1414–1428. [PubMed: 24525631]
10. Piegeler T, Cotta-Velis EG, Liu G, Place AT, Schwartz DE, Beck-Schimmer B, Minshall RD, Borgeat A. Antimetastatic Potential of Amide-linked Local Anesthetics: Inhibition of Lung Adenocarcinoma Cell Migration and Inflammatory Src Signaling Independent of Sodium Channel Blockade. Anesthesiology. 2012; 117:548–559. [PubMed: 22846676]

11. Lu J, Xu SY, Zhang QG, Lei HY. Bupivacaine induces reactive oxygen species production via activation of the AMP-activated protein kinase-dependent pathway. Pharmacology. 2011; 87:121–129. [PubMed: 21304223]
12. Huang L, Kondo F, Gosho M, Feng G-G, Harato M, Xia Z, Ishikawa N, Fujiwara Y, Okada S. Enhanced expression of WD repeat-containing protein 35 via CaMKK/AMPK activation in bupivacaine-treated Neuro2a cells. PLoS One. 2014; 9:98185.
13. Lee SJ, Shin TJ, Kang IS, Ha JH, Lee SC, Kim HJ. AMPK attenuates bupivacaine-induced neurotoxicity. J. Dent. Res. 2010; 89:797–801. [PubMed: 20448244]
14. Rahman S, Li J, Bopassa JCJ, Umar S, Iorga A, Partownavid P, Eghbali M. Phosphorylation of GSK-3b Mediates Intralipid-induced Cardioprotection against Ischemia/Reperfusion Injury. Anesthesiology. 2011; 115:242–253. [PubMed: 21691195]
15. Li J, Iorga A, Sharma S, Youn J-Y, Partow-Navid R, Umar S, Cai H, Rahman S, Eghbali M. Intralipid, a Clinically Safe Compound, Protects the Heart Against Ischemia-Reperfusion Injury More Efficiently Than Cyclosporine-A. Anesthesiology. 2012; 117:836–846. [PubMed: 22814384]
16. Lou P-H, Lucchinetti E, Zhang L, Affolter A, Schaub MC, Gandhi M, Hersberger M, Warren BE, Lemieux H, Sobhi HF, Clanachan AS, Zaugg M. The mechanism of Intralipid®-mediated cardioprotection complex IV inhibition by the active metabolite, palmitoylcarnitine, generates reactive oxygen species and activates reperfusion injury salvage kinases. PLoS One. 2014; 9:87205.
17. Li J, Fettiplace MR, Chen S-J, Steinhorn B, Shao Z, Zhu X, Li C, Harty S, Weinberg G, Hoek TL Vanden. Lipid Emulsion Rapidly Restores Contractility in Stunned Mouse Cardiomyocytes: A Comparison With Therapeutic Hypothermia. Crit Care Med. 2014; 42:734–740.
18. Zirpoli H, Abdillahi M, Quadri N, Ananthakrishnan R, Wang L, Rosario R, Zhu Z, Deckelbaum RJ, Ramasamy R. Acute Administration of n-3 Rich Triglyceride Emulsions Provides Cardioprotection in Murine Models after Ischemia-Reperfusion. PLoS One. 2015; 10:0116274.
19. Anavi S, Ilan E, Tirosh O, Madar Z. Infusion of a lipid emulsion modulates AMPK and related proteins in rat liver, muscle, and adipose tissues. Obesity. 2010; 18:1108–1115. [PubMed: 20057367]
20. Weinberg GL, Ripper R, Murphy P, Edelman LB, Hoffman W, Strichartz G, Feinstein DL. Lipid infusion accelerates removal of bupivacaine and recovery from bupivacaine toxicity in the isolated rat heart. Reg Anesth Pain Med. 2006; 31:296–303. [PubMed: 16857549]
21. Coyle DE, Sperelakis N. Bupivacaine and lidocaine blockade of calcium-mediated slow action potentials in guinea pig ventricular muscle. J Pharmacol Exp Ther. 1987; 242:1001–1005. [PubMed: 2443640]
22. Clarkson C, Hondeghem L. Mechanism for Bupivacaine Depression of Cardiac Conduction: Fast Block of Sodium Channels during the Action Potential with Slow Recovery from Block during Diastole. Anesthesiology. 1985; 62:396–405. [PubMed: 2580463]
23. Terasaki T, Pardridge WM, Denson DD. Differential effect of plasma protein binding of bupivacaine on its in vivo transfer into the brain, salivary gland of rats. J. Pharmacol. Exp. Ther. 1986; 239:724–729. [PubMed: 3795038]
24. Conover WJ, Iman RL. Rank Transformation as a Bridge Between Parametric, Nonparametric Statistics. Am. Stat. Assoc. 1981; 35:124–129.
25. Akritas MG. Method in Some The Rank Transform Two-Factor Designs. Am. Stat. Assoc. 1990; 85:73–78.
26. Fettiplace MR, Ripper R, Lis K, Feinstein DL, Rubinstein I, Weinberg G. Intraosseous Lipid Emulsion: An Effective Alternative to IV Delivery in Emergency Situations. Crit Care Med. 2014; 42:157–160.
27. Ravichandran LV, Esposito DL, Chen J, Quon MJ. Protein kinase C-zeta phosphorylates insulin receptor substrate-1, impairs its ability to activate phosphatidylinositol 3-kinase in response to insulin. J. Biol. Chem. 2001; 276:3543–3549. [PubMed: 11063744]
28. Pereira S, Park E, Mori Y, Haber CA, Han P, Uchida T, Stavar L, Oprescu AI, Koulajian K, Ivovic A, Yu Z, Li D, Bowman TA, Dewald J, El-Benna J, Brindley DN, Gutierrez-Juarez R, Lam TKT, Najjar SM, McKay Ra, Bhanot S, Fantus IG, Giacca A. FFA-induced hepatic insulin resistance in

vivo is mediated by PKC-δ, NADPH oxidase, and oxidative stress. Am J Physiol Endocrinol Metab. 2014; 307:e34–e46. [PubMed: 24824652]

29. Moschella PC, Rao VU, McDermott PJ, Kuppuswamy D. Regulation of mTOR, S6K1 activation by the nPKC isoforms, PKCepsilon PKCdelta in adult cardiac muscle cells. J. Mol. Cell. Cardiol. 2007; 43:754–766. [PubMed: 17976640]
30. Witczak, Ca; Sharoff, CG.; Goodyear, LJ. AMP-activated protein kinase in skeletal muscle: From structure localization to its role as a master regulator of cellular metabolism. Cell. Mol. Life Sci. 2008; 65:3737–3755. [PubMed: 18810325]
31. Scheuer J, Stezoski SW. Protective role of increased myocardial glycogen stores in cardiac anoxia in the rat. Circ. Res. 1970; 27:835–849. [PubMed: 5486250]
32. Russell R, Li J, Coven D, Pypaert M, Zechner C, Palmeri M, Giordano F, Mu J, Birnbaum M, Young L. AMP-activated protein kinase mediates ischemic glucose uptake and prevents postischemic cardiac dysfunction, apoptosis, and injury. J Clin Invest. 2004; 114:495–503. [PubMed: 15314686]
33. Fettiplace MR, Weinberg G. Should transient physiologic effects following lipid administration be attributed to a cellular signaling mechanism without cellular data? Crit Care Med. 2013:41. Author reply. [PubMed: 23222263]
34. Wong GK, Crawford MW. Carnitine deficiency increases susceptibility to bupivacaine-induced cardiotoxicity in rats. Anesthesiology. 2011; 114:1417–1424. [PubMed: 21537157]
35. Weinberg GL, Laurito CE, Geldner P, Pygon BH, Burton BK. Malignant Ventricular Dysrhythmias in a Patient with Isovaleric Acidemia Receiving General and Local Anesthesia for Suction Lipectomy. J Clin Anesth. 1997; 9:668–670. [PubMed: 9438897]
36. Wong GK, Joo DT, McDonnell C. Lipid resuscitation in a carnitine deficient child following intravascular migration of an epidural catheter. Anaesthesia. 2010; 65:192–195. [PubMed: 19849674]
37. Weinberg GL, Palmer JW, VadeBoncouer TR, Zuechner MB, Edelman G, Hoppel CL. Bupivacaine Inhibits Acylcarnitine Exchange in Cardiac Mitochondria. Anesthesiology. 2000; 92:523–528. [PubMed: 10691241]
38. Fettiplace MR, Pichurko A, Ripper R, Lin B, Kowal K, Lis K, Schwartz D, Feinstein DL, Rubinstein I, Weinberg G. Cardiac Depression Induced by Cocaine or Cocaethylene Is Alleviated by Lipid Emulsion More Effectively Than by Sulfobutylether-β-cyclodextrin. Acad Emerg Med. 2015; 22:508–517. [PubMed: 25908403]
39. Eledjam JJ, La Coussaye JE de, Brugada J, Bassoul B, Gagnol JP, Fabregat JR, Massé C, Sassine A. In vitro study on mechanisms of bupivacaine-induced depression of myocardial contractility. Anesth Analg. 1989; 69:732–735. [PubMed: 2589652]
40. Imai M, Chang K, Tanz R, Stevens W, Kemmotsu O. [Enhanced myocardial depression from bupivacaine in diabetic rats] (Article in Japanese). Masui. 1991; 40:1991.
41. Lu GP, Schwalbe SS, Marx GF, Batiller G, Limjoco R. Hypoglycemia enhances bupivacaine-induced cardiotoxicity in the rat. J. Anesth. 1992; 6:255–261. [PubMed: 15278534]
42. Stehr SN, Pexa A, Hannack S, Heintz A, Heller a R, Deussen A, Koch T, Hübler M. Insulin effects on myocardial function, bioenergetics in L-bupivacaine toxicity in the isolated rat heart Eur. J. Anaesthesiol. 2007; 24:340–346.
43. Kim J-T, Jung C-W, Lee K-H. The effect of insulin on the resuscitation of bupivacaine-induced severe cardiovascular toxicity in dogs. Anesth Analg. 2004; 99:728–733. [PubMed: 15333402]
44. Lirk P, Flatz M, Haller I, Hausott B, Blumenthal S, Stevens M, Suzuki S, Klimaschewski L, Gerner P. In Zucker Diabetic Fatty Rats, Subclinical Diabetic Neuropathy Increases In Vivo Lidocaine Block Duration But Not In Vitro Neurotoxicity. Reg Anesth Pain Med. 2012; 37:601–606. [PubMed: 23011115]
45. Lirk P, Verhamme C, Boeckh R, Stevens MF, Ten Hoope W, Gerner P, Blumenthal S, de Girolami U, van Schaik IN, Hollmann MW, Picardi S. Effects of early and late diabetic neuropathy on sciatic nerve block duration and neurotoxicity in Zucker diabetic fatty rats. Br J Anaesth. 2015; 114:319–326. [PubMed: 25145353]

46. Kroin JS, Buvanendran A, Tuman KJ, Kerns JM. Effect of acute versus continuous glycemic control on duration of local anesthetic sciatic nerve block in diabetic rats. Reg Anesth Pain Med. 2012; 37:595–600. [PubMed: 22996200]
47. Kalichman M, Calcutt N. Local Anesthetic-induced Conduction Block and Nerve Fiber Injury in Streptozotocin-Diabetic Rats. Anesthesiology. 1992; 77:1992.
48. Cuvillon P, Reubrecht V, Zoric L, Lemoine L, Belin M, Ducombs O, Birenbaum A, Riou B, Langeron O. Comparison of subgluteal sciatic nerve block duration in type 2 diabetic, non-diabetic patients. Br. J. Anaesth. 2013; 110:823–830. [PubMed: 23348203]
49. Sertoz N, Deniz MN, Ayanoglu HO. Relationship between glycosylated hemoglobin level and sciatic nerve block performance in diabetic patients. Foot ankle Int. 2013; 34:85–90. [PubMed: 23386766]
50. Gebhard RE, Nielsen KC, Pietrobon R, Missair A, Williams Ba. Diabetes mellitus, independent of body mass index, is associated with a “higher success” rate for supraclavicular brachial plexus blocks. Reg Anesth Pain Med. 2009; 34:404–407. [PubMed: 19920415]
51. Williams BA, Murinson BB, Grable BR, Orebaugh SL. Future considerations for pharmacologic adjuvants in single-injection peripheral nerve blocks for patients with diabetes mellitus. Reg Anesth Pain Med. 2009; 34:445–457. [PubMed: 19920420]
52. Sugden PH, Fuller SJ, Weiss SC, Clerk A. Glycogen synthase kinase 3 (GSK3) in the heart: a point of integration in hypertrophic signalling and a therapeutic target? A critical analysis. Br. J. Pharmacol. 2008; (153 Suppl):137–153.
53. Kirk JA, Holewinski RJ, Kooij V, Agnetti G, Tunin RS, Witayavanitkul N, Tombe PP De, Gao WD, Eyk J Van, Kass DA. Cardiac resynchronization sensitizes the sarcomere to calcium by reactivating GSK-3 β. J Clin Invest. 2014; 124:129–139. [PubMed: 24292707]
54. Gao MH, Tang T, Guo T, Miyanohara A, Yajima T, Pestonjamasp K, Feramisco JR, Hammond HK. Adenylyl cyclase type VI increases Akt activity and phospholamban phosphorylation in cardiac myocytes. J Biol Chem. 2008; 283:33527–33535. [PubMed: 18838385]
55. Cittadini, a; Monti, MG.; Iaccarino, G.; Rella, F Di; Tsichlis, PN.; Gianni, A Di; Strömer, H.; Sorriento, D.; Peschle, C.; Trimarco, B.; Saccà, L.; Condorelli, G. Adenoviral gene transfer of Akt enhances myocardial contractility and intracellular calcium handling. Gene Ther. 2006; 13:8–19. [PubMed: 16094411]
56. Ross J, Ripper R, Law W, MAssa M, Murphy P, Edelman L, Conlon B, Feinstein DL, Palmer JW, DiGregorio G, Weinberg GL. Adding bupivacaine to high-potassium cardioplegia improves function and reduces cellular damage of rat isolated hearts after prolonged, cold storage. Anesthesiology. 2006; 105:746–752. [PubMed: 17006074]
57. Bouwman RA, Vreden MJa, Hamdani N, Wassenaar LEJ, Smeding L, Loer Sa, Stienen GJM, Lamberts RR. Effect of bupivacaine on sevoflurane-induced preconditioning in isolated rat hearts. Eur. J. Pharmacol. 2010; 647:132–138. [PubMed: 20816812]
58. Taftachi F, Sanaei-Zadeh H, Sepehrian B, Zamani N. Lipid emulsion improves Glasgow Coma Scale, decreases blood glucose level in the setting of acute non-local anesthetic drug poisoning - A randomized controlled trial. Eur. Rev. Med. Pharmacol. Sci. 2012; 16:38–42. [PubMed: 22582483]
59. Hiller DB, Gregorio G Di, Ripper R, Kelly K, Massad M, Edelman L, Edelman G, Feinstein DL, Weinberg GL. Epinephrine Impairs Lipid Resuscitation from Bupivacaine Overdose: A Threshold Effect. Anesthesiology. 2009; 111:498–505. [PubMed: 19704251]
60. Hiller N, Mirtschink P, Merkel C, Knels L, Oertel R, Christ T, Deussen A, Koch T, Stehr SN. Myocardial accumulation of bupivacaine, ropivacaine is associated with reversible effects on mitochondria, reduced myocardial function. Anesth. Analg. 2013; 116:83–92. [PubMed: 23223114]
61. Holger J, Engebretsen K, Marini J. High dose insulin in toxic cardiogenic shock. Clin Toxicol. 2009; 47:303–307.
62. Levine M, Boyer EW, Pozner CN, Geib A-J, Thomsen T, Mick N, Thomas SH. Assessment of hyperglycemia after calcium channel blocker overdoses involving diltiazem or verapamil*. Crit Care Med. 2007; 35:2071–2075. [PubMed: 17855820]

63. Boyer EW, Duic Pa, Evans A. Hyperinsulinemia/euglycemia therapy for calcium channel blocker poisoning. Ped Emerg Care. 2002; 18:36–37.

64. Bechtel LK, Haverstick DM, Holstege CP. Verapamil toxicity dysregulates the phosphatidylinositol 3-kinase pathway. Acad Emerg Med. 2008; 15:368–374. [PubMed: 18370992]

65. Benzeroual K, Pandey S, Srivastava A, Werve G, Van de Haddad P. Insulin-induced Ca(2+) entry in hepatocytes is important for PI 3-kinase activation , but not for insulin receptor and IRS-1 tyrosine. Biochim Biophys Acta. 2000; 1495:14–23. [PubMed: 10634928]

66. Khoza S, Barner JC. Glucose dysregulation associated with antidepressant agents an analysis of 17 published case reports. Int J Clin Pharm. 2011; 33:484–492. [PubMed: 21487738]

67. Weber-Hamann B, Gilles M, Lederbogen F, Heuser I, Deuschle M. Improved Insulin Sensitivity in 80 Nondiabetic Patients With MDD After Clinical Remission in a Double-Blind, Randomized Trial of Amitriptyline and Paroxetine. J Clin Psychiatry. 2006; 67:1857–1862.

68. Kerns W. Management of beta-adrenergic blocker and calcium channel antagonist toxicity. Emerg Med Clin N Am. 2007; 25:309–331.

69. Carley AN, Bi J, Wang X, Banke NH, Dyck JRB, O'Donnell JM, Lewandowski ED. Multiphasic triacylglycerol dynamics in the intact heart during acute in vivo overexpression of CD36. J Lipid Res. 2013; 54:97–106. [PubMed: 23099442]

70. Lahey R, Wang X, Carley aN, Lewandowski ED. Dietary Fat Supply to Failing Hearts Determines Dynamic Lipid Signaling for Nuclear Receptor Activation and Oxidation of Stored Triglyceride. Circulation. 2014; 130:1790–1799. [PubMed: 25266948]

71. Carley AN, Taegtmeyer H, Lewandowski ED. Matrix revisited: mechanisms linking energy substrate metabolism to the function of the heart. Circ. Res. 2014; 114:717–729. [PubMed: 24526677]

72. Liang CW, Diamond SJ, Hagg DS. Lipid rescue of massive verapamil overdose: a case report. J Med Case Rep. 2011; 5:399. [PubMed: 21854635]

73. Tebbutt S, Harvey M, Nicholson T, Cave G. Intralipid prolongs survival in a rat model of verapamil toxicity. Acad. Emerg. Med. 2006; 13:134–139. [PubMed: 16436797]

74. Bania TC, Chu J, Perez E, Su M, Hahn IH. Hemodynamic Effects of Intravenous Fat Emulsion in an Animal Model of Severe Verapamil Toxicity Resuscitated with Atropine, Calcium Saline. Acad. Emerg. Med. 2007; 14:105–111. [PubMed: 17267527]

75. Harvey M, Cave G. Intralipid outperforms sodium bicarbonate in a rabbit model of clomipramine toxicity. Ann Emerg Med. 2007; 49:178–185. 185.e1–4. [PubMed: 17098328]

76. Engels PT, Davidow JS. Intravenous fat emulsion to reverse haemodynamic instability from intentional amitriptyline overdose. Resuscitation. 2010; 81:1037–1039. [PubMed: 20605670]

77. Harvey M, Cave G, Lahner D, Desmet J, Prince G, Hopgood G. Insulin versus Lipid Emulsion in a Rabbit Model of Severe Propranolol Toxicity: A Pilot Study. Crit. Care Res. Pract. 2011; 2011:361737. [PubMed: 21541209]

Summary Statement

Insulinergic signaling is uncoupled during local anesthetic cardiotoxicity then becomes sensitized during recovery. The latter effect is potentiated by lipid infusion. This offers novel explanations for bupivacaine toxicity, the biochemical responses underlying spontaneous recovery of physiologic homeostasis and the benefit of lipid infusion.

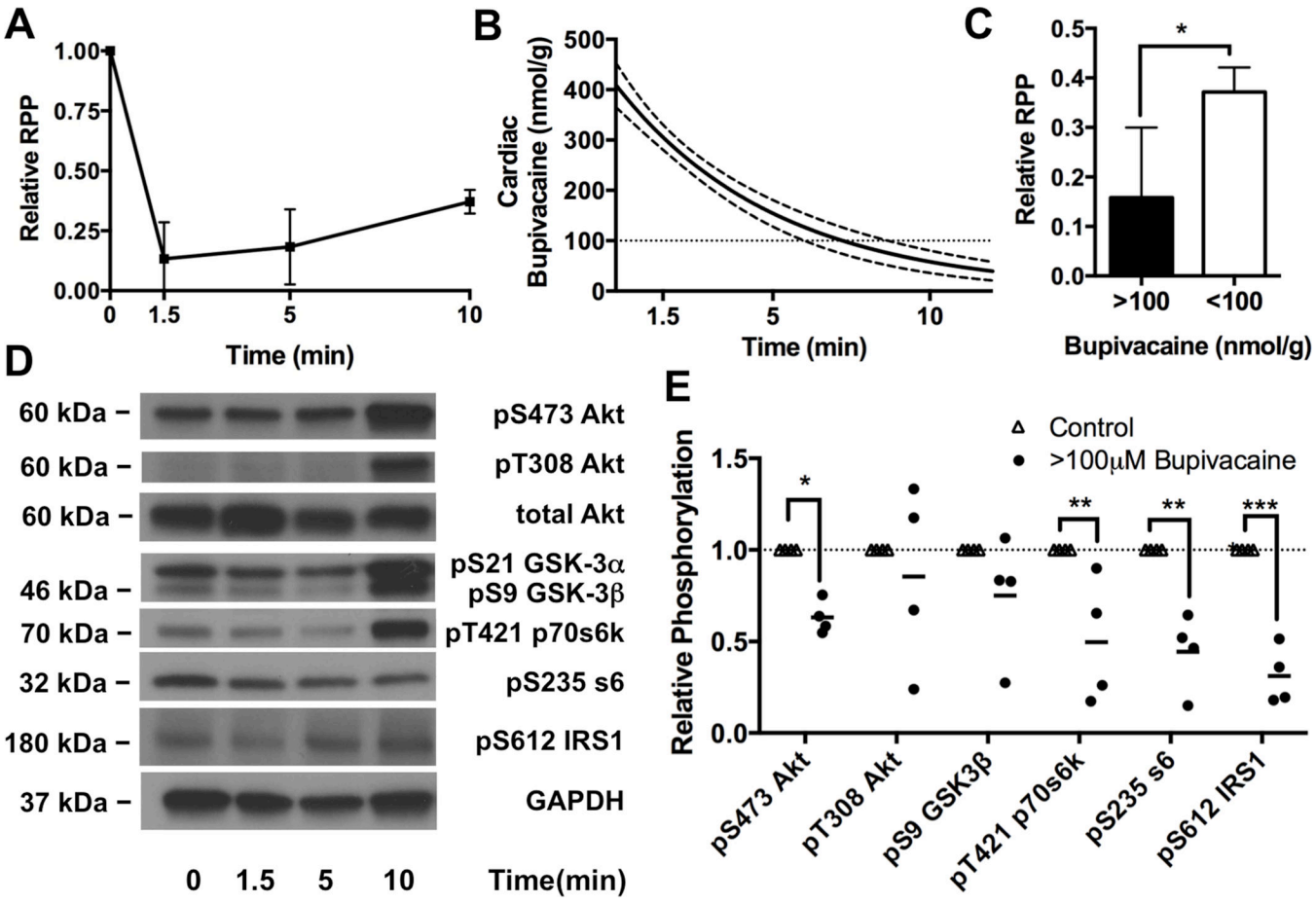

Figure 1. Cardiac phosphorylation of Protein kinase B/Akt and downstream proteins following bupivacaine toxicity

A. Cardiac output as measured by rate-pressure-product (RPP = mean arterial pressure x heart rate) in response to bupivacaine toxicity. **B**. Theoretical cardiac bupivacaine (solid line) concentration with 95% confidence interval (dotted lines) based on radiolabel studies (see "Methods: Bupivacaine concentration fit curves & grouping") **C**. Relative RPP difference between groups above ionotropic cation channel (e.g. sodium & calcium) IC_{50} (>100μm bupivacaine) and below cation channel IC_{50} (<100 μM bupivacaine), *:p<0.05 **D**. Western blots of cardiac lysates at different time-points during recovery for phospho-proteins in the insulinergic pathway including protein kinase B (Akt) phosphorylated at S473, Akt phosphorylated at T308, total Akt, glycogen synthase kinase alpha (GSK-3α) and beta (GSK-3β) phosphorylated at S21 and S9 respectively, p70 s6 kinase (p70s6k) phosphorylated at T421, ribosomal protein s6 (s6) phosphorylated at S235, Insulin receptor substrate 1 (IRS1) phosphorylated at S612, and total glyceraldehyde-3-phosphate dehydrogenase (GAPDH) as loading control. **E**. Densitometry of cardiac lysates (from "D") comparing control phosphorylation (n=4) to unrecovered animals with >100μM of cardiac bupivacaine (n=4); *p<0.05, **p<0.01,***p<0.001, Sidak post-hoc test.

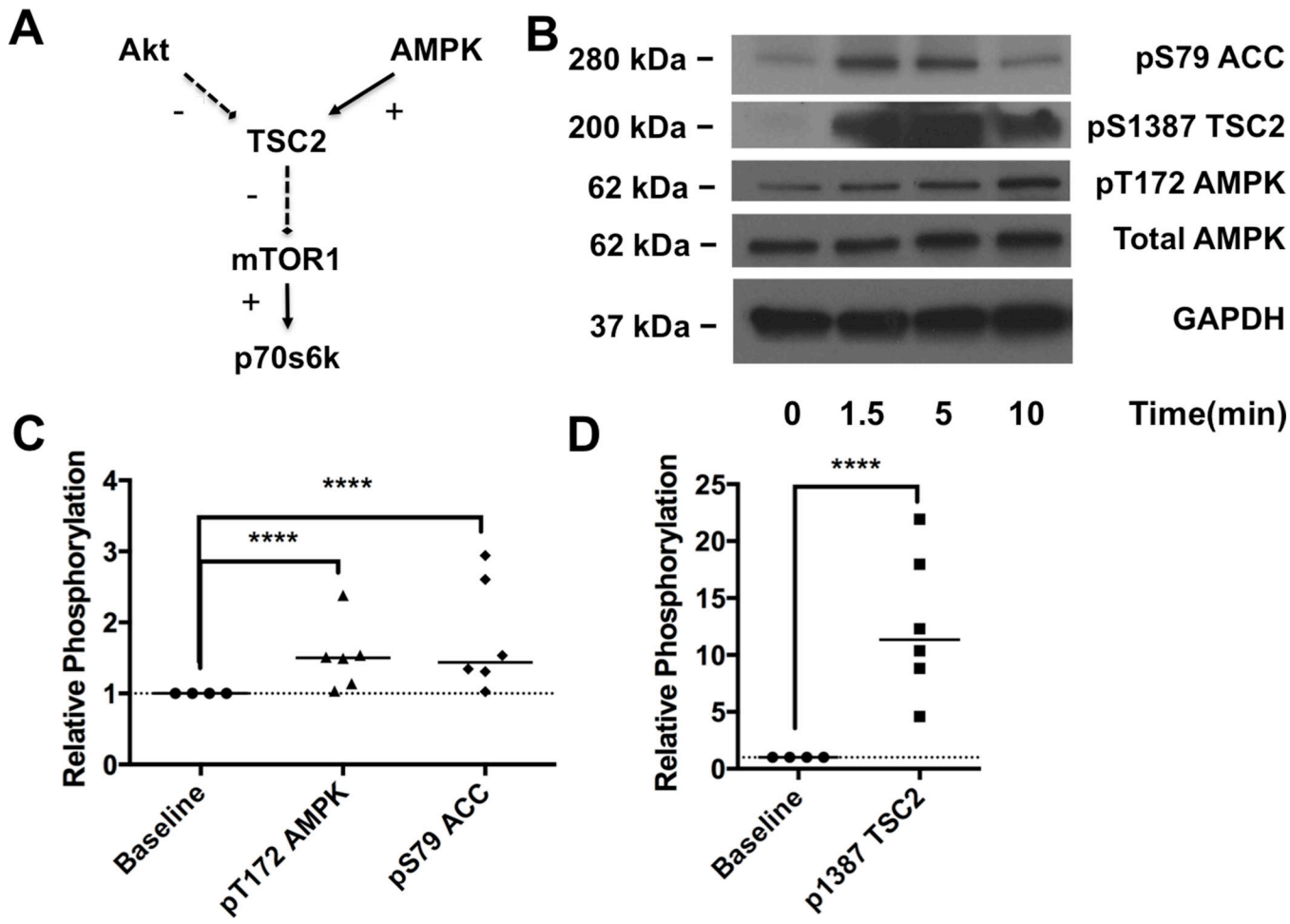

Figure 2. 5' adenosine monophosphate activated kinase phosphorylation during toxicity

A. Cellular signaling schematic illustrating the convergence of protein kinase B (Akt) and 5' adenosine monophosphate activated kinases (AMPK) signaling on the mammalian target of rapamycin complex 1 (mTOR1) which controls downstream targets including p70 s6 kinase (p70s6k). **B**. Western blots of cardiac lysates at different time-points during recovery for the AMPK pathway including acetyl CoA carboxylase (ACC) phosphorylated at S79, tuberous sclerosis 2 (TSC2) phosphorylated at S1387, AMPK phosphorylated at T172, total AMPK and total glyceraldehyde-3-phosphate dehydrogenase (GAPDH) as loading control **C**. Densitometry of phospho-AMPK and phospho-ACC comparing concentrations at baseline (n=4) to concentrations during toxicity (n=6); ****p<0.0001, post-hoc Sidak test. **D**. Densitometry of phospho-TSC2 comparing concentrations at baseline (n=4) to concentrations during toxicity (n=6); *p<0.0001, Sidak post-hoc test.

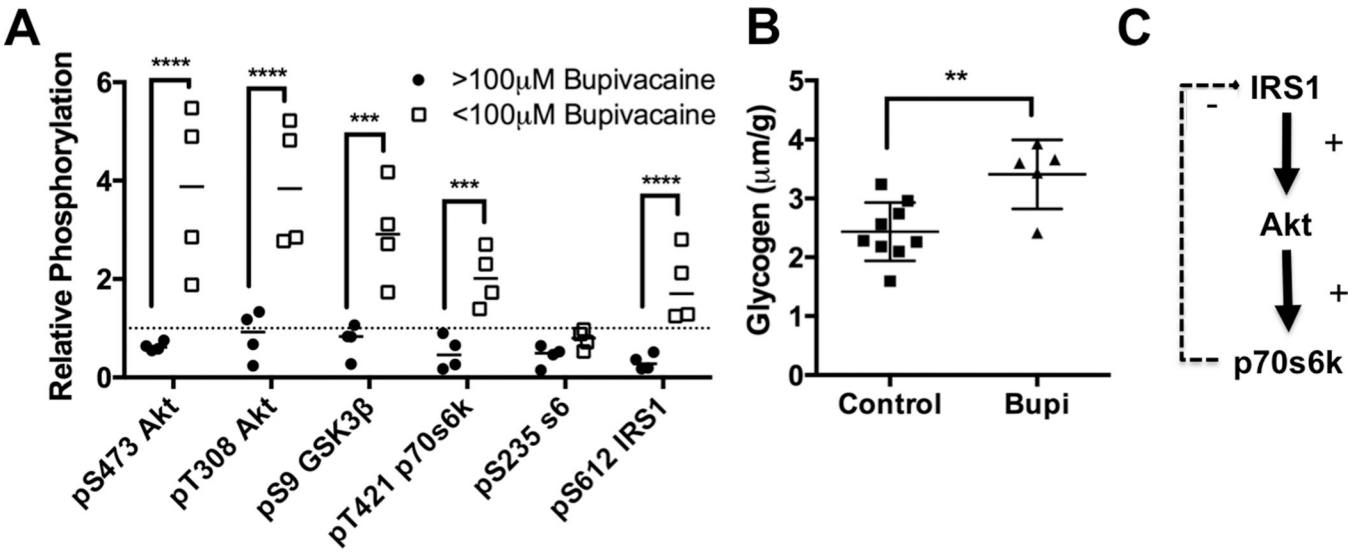

Figure 3. Recovery dependent cardiac protein phosphorylation

A. Densitometry of phospho-proteins in insulinergic pathway in recovered animals with <100μM cardiac bupivacaine (n=4) compared to densitometry during toxicity (>100μM bupivacaine, n=4); ***p<0.001, ****p<0.0001, Sidak post-hoc test. Proteins blotted for include protein kinase B (Akt) phosphorylated at S473, Akt phosphorylated and T308, total Akt, glycogen synthase kinase alpha (GSK-3α) and beta (GSK-3β) phosphorylated at S21 and S9 respectively, p70 s6 kinase (p70s6k) phosphorylated at T421, ribosomal protein s6 (s6) phosphorylated at S235, insulin receptor substrate 1 (IRS1) phosphorylated at S612, and total glyceraldehyde-3-phosphate dehydrogenase (GAPDH) as loading control. **B**. Cardiac glycogen concentration for control hearts (n=9) and bupivacaine treated hearts in recovery (n=5) **:p=0.01 by two-sided t-test. **C**. Schematic of feedback pathway underlying sensitization of insulinergic signaling demonstrating how loss of feedback from p70s6k (and other kinases) to IRS1 leads to a sensitization and amplified activation of downstream targets including Akt.

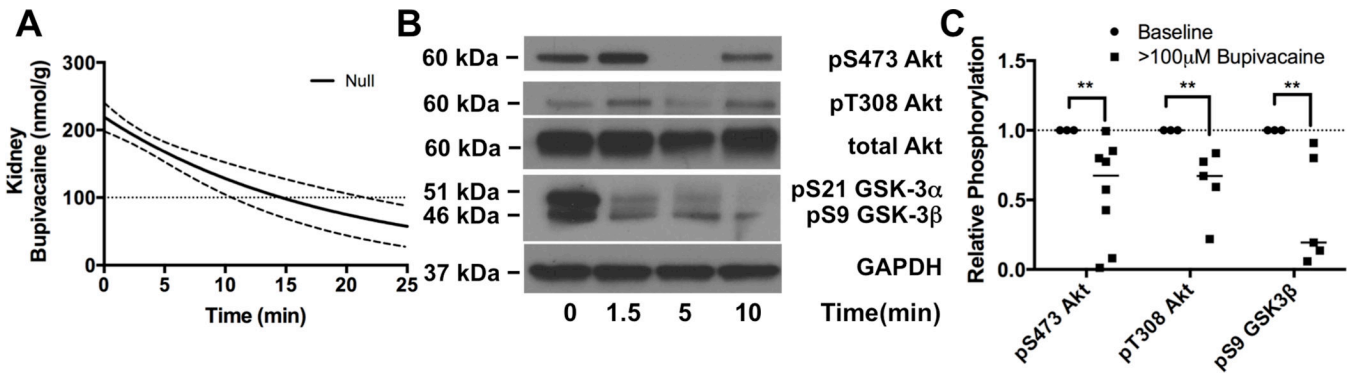

Figure 4. Protein kinase B/Akt & downstream de-phosphorylation is not tissue dependent

A. Theoretical kidney bupivacaine concentration (solid line) with 95% confidence interval (dotted lines) based on radiolabel studies (see "Methods: Bupivacaine concentration fit curves & grouping") **B**. Western blots of lysates from cortex of kidney at different time-points during recovery for protein kinase B (Akt) phosphorylated at S473, Akt phosphorylated at T308, glycogen synthase kinase-3-alpha (GSK-3α) and beta (GSK-3β) phosphorylated at S21 and S9 respectively with total glyceraldehyde-3-phosphate dehydrogenase (GAPDH) as loading control. **C**. Densitometry of kidney lysate western blots for Akt at S473 and T308 relative to total Akt & loading control and densitometry of GSK-3β relative to loading control for tissue concentration of bupivacaine greater than sodium channel IC_{50} (>100μM Bupivacaine) compared to baseline **p<0.01, Sidak post-hoc test.

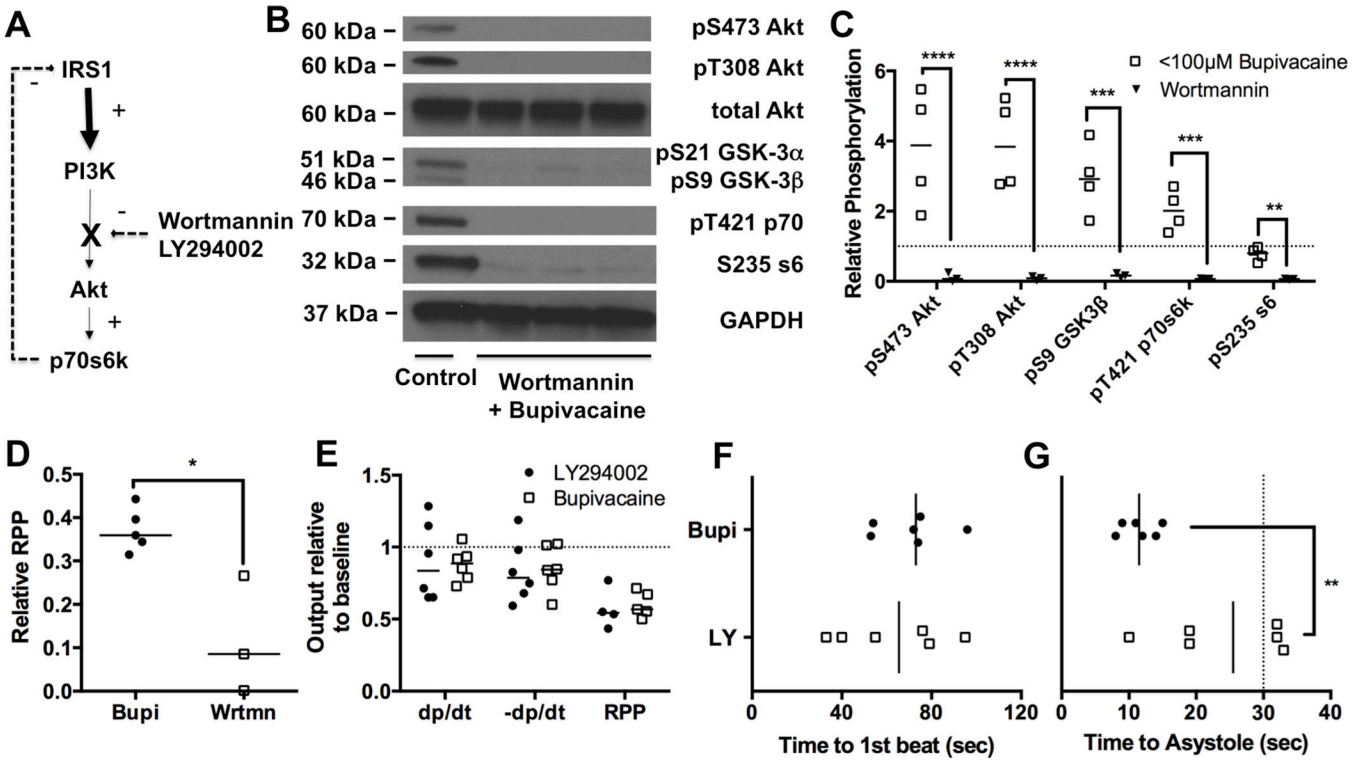

Figure 5. Blocking signaling exacerbates toxicity

A. Simplified schematic of insulinergic signaling from insulin receptor substrate 1 (IRS1) to phosphoinositol-3-kinase (Pi3k) to Protein kinase B (Akt) to p70 s6 kinase (p70s6k) with inhibition point by Wortmannin & LY294002 between Pi3k and Akt. **B**. Western blots of cardiac lysates for 10-minute time-point for animals pre-treated with Wortmannin before bupivacaine infusion. Proteins blotted for include Akt phosphorylated at S473, Akt phosphorylated at T308, total Akt, glycogen synthase kinase alpha (GSK-3α) and beta (GSK-3β)???????????phosphorylated at S21 and S9 respectively, p70 s6 kinase (p70s6k) phosphorylated at T421, ribosomal protein s6 (s6) phosphorylated at S235, and total glyceraldehyde-3-phosphate dehydrogenase (GAPDH) as loading control. **C**. Densitometry of cardiac lysates comparing protein phosphorylation in recovered animals treated with bupivacaine (n=4, <100μM Bupivacaine) or bupivacaine and Wortmannin (n=3, Wortmannin); **p<0.01, ***p<0.001, ****p<0.0001, Sidak post-hoc test **D**. Relative rate-pressure-product (RPP = mean arterial pressure x heart rate) at 10-minutes for animals recovering from bupivacaine toxicity either pretreated with Wortmannin (Wrtmn) or nothing (Bupi); *=p<0.05, Mann-Whitney U-test **E**. Physiological parameters including maximal contraction (dp/dt), maximum relaxation (-dp/dt) and RPP from isolated Langendorff hearts at 2-minute recovery point following treatment with 500μM bupivacaine over 30 seconds. Hearts were either pre-dosed with 50μM LY294002 (LY294002) or nothing (Bupivacaine) **F**. Time to recovery of first beat for hearts from “E” following bupivacaine-induced asystole. **G**. Time to asystole for hearts following bupivacaine treatment for hearts in “E”.

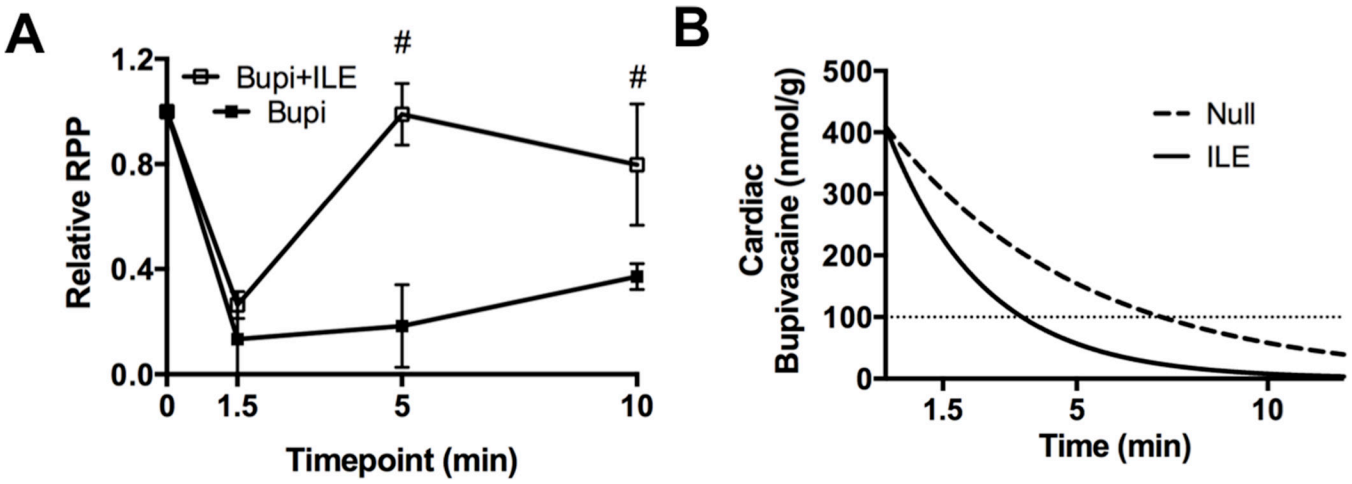

Figure 6. Cardiac pharmacodynamic and pharmacokinetic effects of lipid emulsion on bupivacaine toxicity

A. Relative rate-pressure-product (RPP = mean arterial pressure x heart rate) in response to bupivacaine toxicity with either nothing (Bupi) or adjuvant 10mL/kg lipid emulsion (Bupi +ILE), #=$p<0.05$ Mann-Whitney U-test. **B**. Theoretical cardiac bupivacaine concentration based on previous pharmacokinetic studies for bupivacaine (Null) or bupivacaine & adjuvant lipid emulsion (ILE) (See "Methods: Bupivacaine concentration fit curves & grouping" for more details.)

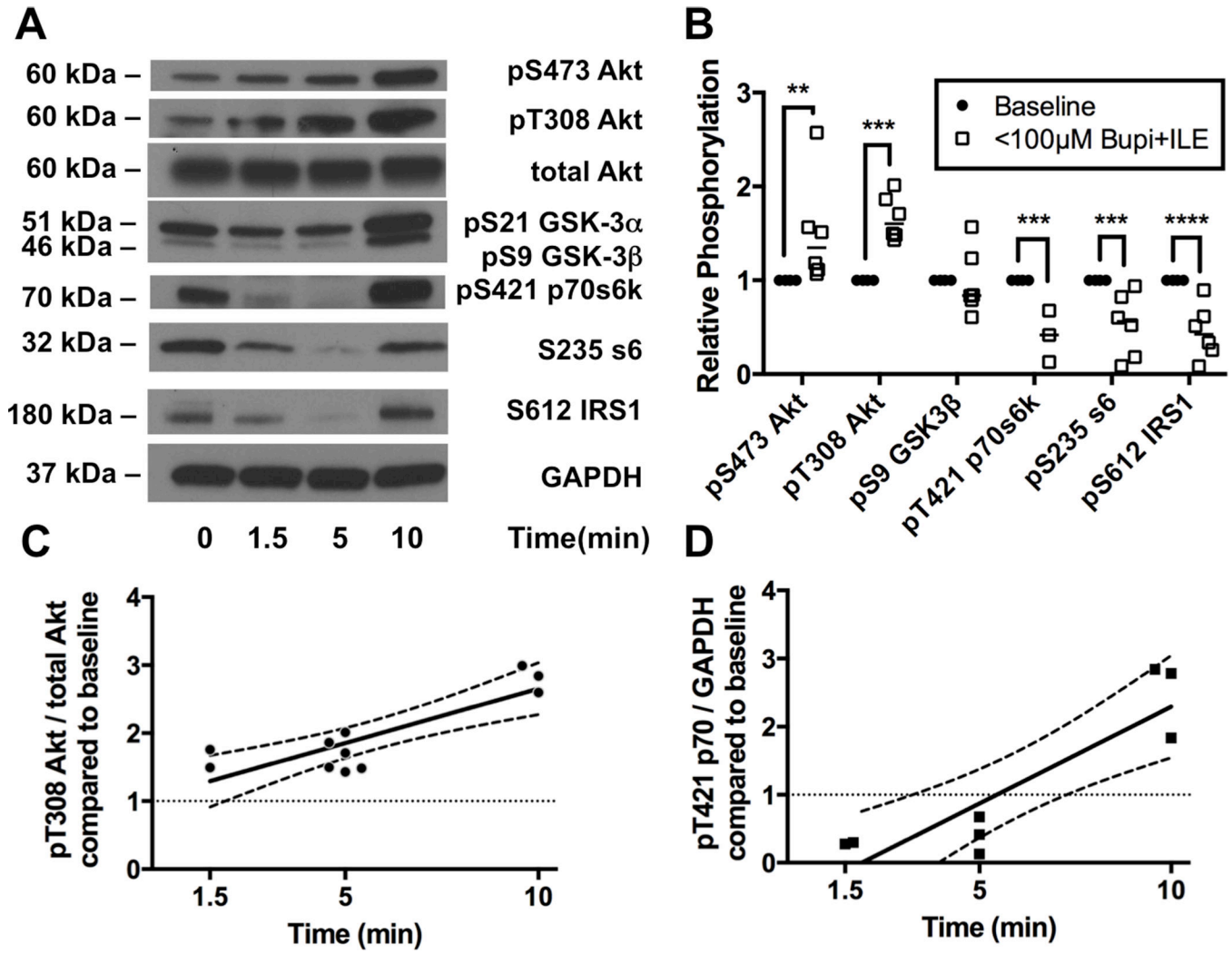

Figure 7. Activation of protein kinase B/Akt upstream of mammalian target of rapamycin in response to bupivacaine & lipid emulsion

A. Western blots of cardiac lysates at different time-points during recovery from bupivacaine toxicity with adjuvant lipid emulsion (ILE) for targets in the insulinergic pathway. Proteins blotted for include protein kinase B (Akt) phosphorylated at S473, Akt phosphorylated at T308, total Akt, glycogen synthase kinase alpha (GSK-3α) and beta (GSK-3β) phosphorylated at S21 and S9 respectively, p70 s6 kinase (p70s6k) phosphorylated at T421, ribosomal protein s6 (s6) phosphorylated at S235, insulin receptor substrate 1 (IRS1) phosphorylated at S612, and total glyceraldehyde-3-phosphate dehydrogenase (GAPDH) as loading control. **B**. Densitometry of cardiac lysates comparing relative phosphorylation level at baseline (n=4) to the relative phosphorylation at the 5-minute time-point (following both bupivacaine & ILE) when animals are recovered and tissue concentrations are expected to be below sodium channel IC_{50} (<100μM Bupi+ILE; n=6; n=3 for p70s6k); **p<0.01, ***p<0.001, ****p<0.0001, Sidak post-hoc test **C**. Regression across time of relative phosphorylation level of threonine 308 on Akt. Fit line: pT308-Akt = 0.16 ± 0.03 * time + 1.0 ± 0.2 R = 0.85. **D**. Regression across time of relative

phosphorylation level of threonine 421 on p70s6k. Fit line: pS421-p70s6k = 0.28 ± 0.06 * time - 0.55 ± 0.4 R = 0.89.

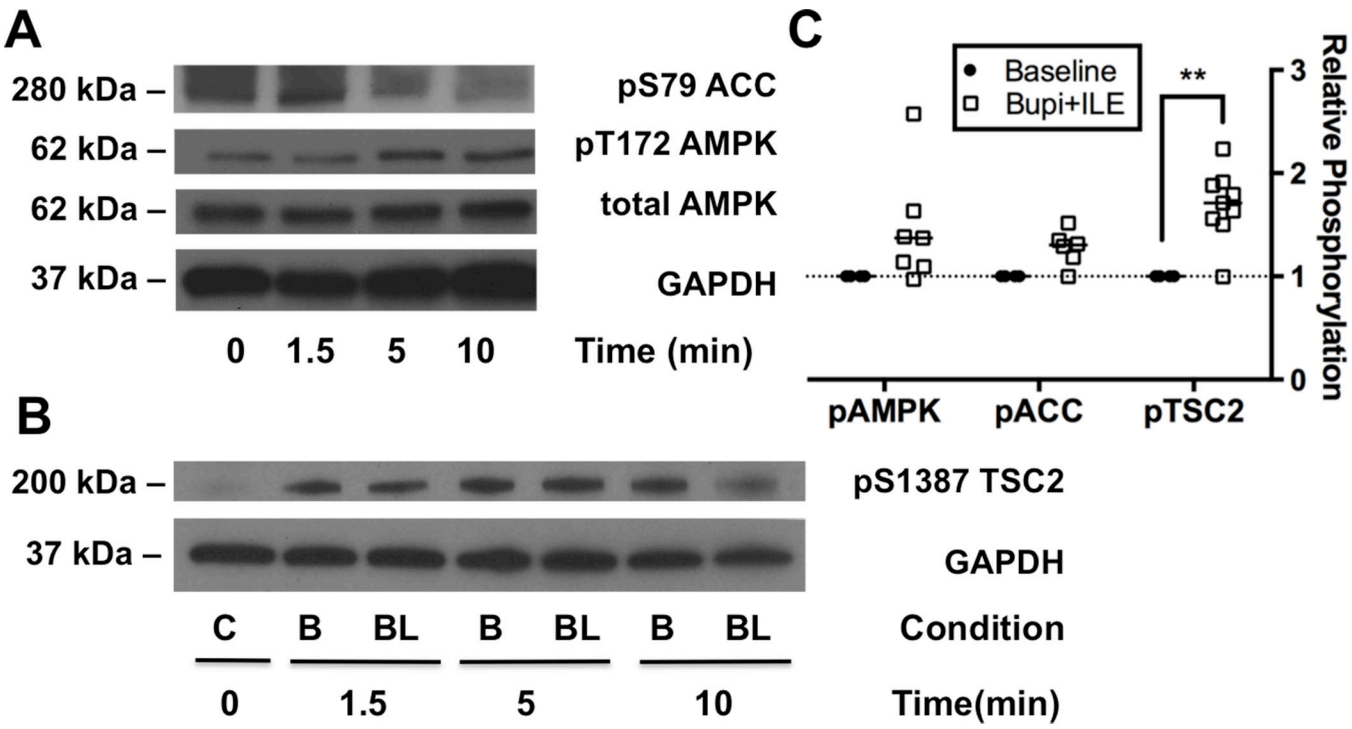

Figure 8. Persistent activation of 5' adenosine monophosphate protein activated kinase signaling despite removal of bupivacaine

A. Western blots of cardiac lysates at different time-points during recovery from toxicity with adjuvant lipid emulsion (ILE) for acetyl-CoA carboxylase (ACC) phosphorylated at S79, 5' adenosine monophosphate activated protein kinase (AMPK) phosphorylated at T172, total AMPK and total glyceraldehyde-3-phosphate dehydrogenase (GAPDH) as loading control. **B**. Western blots of tuberous sclerosis 2 (TSC2) phosphorylated at S1387 and total GAPDH as loading control from cardiac lysates at different time-points during recovery from toxicity with bupivacaine (condition = B) and with bupivacaine and adjuvant ILE (Condition = BL). **C**. Densitometry of phospho-proteins from cardiac lysates comparing relative phosphorylation level of baseline with samples treated with bupivacaine & adjuvant ILE (bupi+ILE; n=7 for pAMPK & pACC, n=9 for pTSC2); **p<0.01, Sidak post-hoc test.

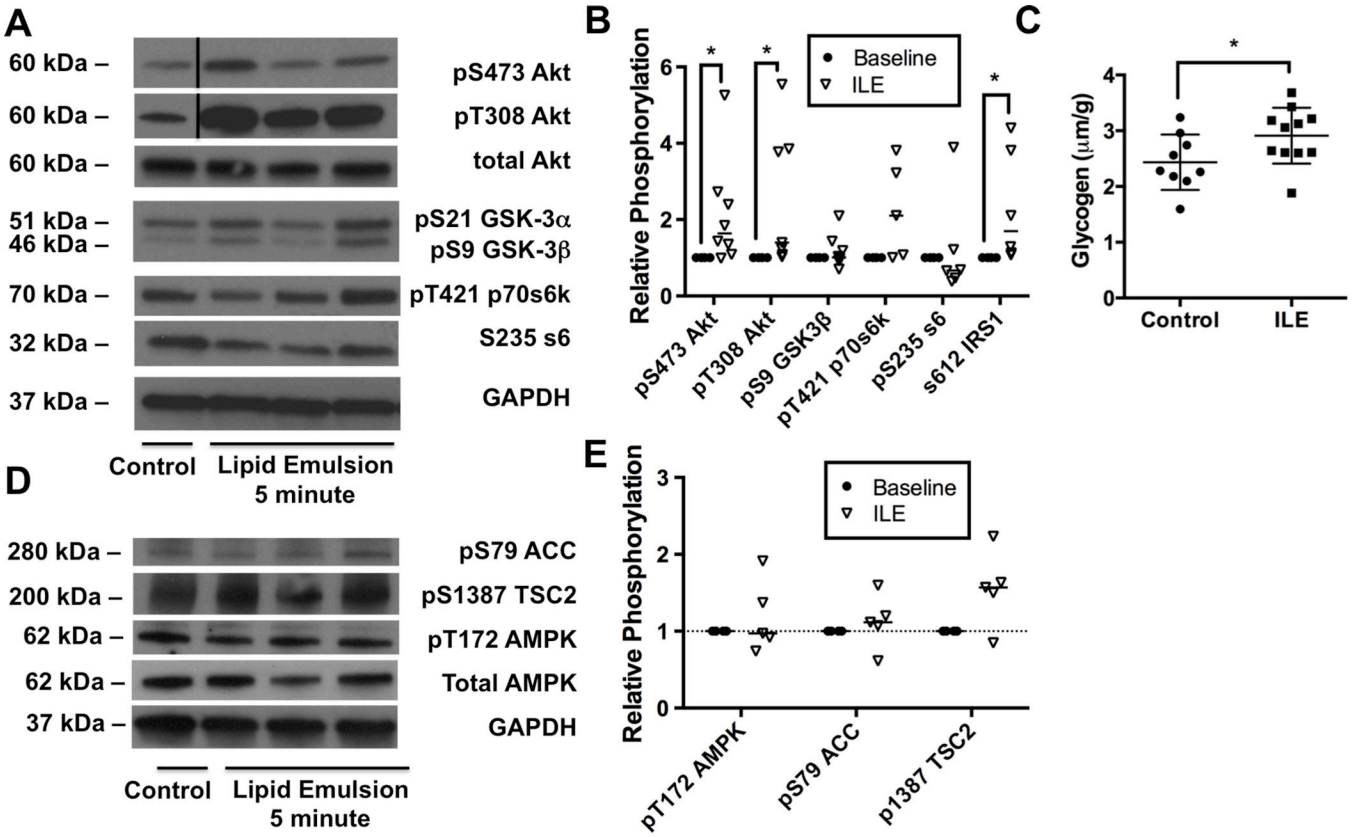

Figure 9. Rapid activation of insulinergic signaling in response to lipid emulsion in the absence of toxicity

A. Western blots for targets in the insulinergic pathway from cardiac lysates 3.5-minutes following 10mL/kg lipid emulsion (ILE, equivalent to 5-minute time-point in bupivacaine + ILE condition). Proteins blotted for include protein kinase B (Akt) phosphorylated at S473, Akt phosphorylated at T308, total Akt, glycogen synthase kinase alpha (GSK-3α) and beta (GSK-3β) phosphorylated at S21 and S9 respectively, p70 s6 kinase (p70s6k) phosphorylated at T421, ribosomal protein s6 (s6) phosphorylated at S235, insulin receptor substrate 1 (IRS1) phosphorylated at S612, and total glyceraldehyde-3-phosphate dehydrogenase (GAPDH) as loading control. **B**. Densitometry of cardiac lysates for data in "A" (n=5–8); *p<0.05, Sidak post-hoc test **C**. Cardiac glycogen concentration for control hearts (n=9) and ILE-treated hearts (n=11) *:p=0.0473 by two-sided t-test. **D**. Western blots for phospho-proteins in the 5' adenosine monophosphate activated protein kinase (AMPK) signaling pathway from cardiac lysates 3.5-minutes following 10mL/kg lipid emulsion (no bupivacaine). Proteins blotted for include AMPK phosphorylated at T172, acetyl-CoA carboxylase (ACC) phosphorylated at S79, tuberous sclerosis 2 (TSC2) phosphorylated at S1387, total AMPK, and total GAPDH as loading control. **E**. Densitometry of cardiac lysates from "D" comparing relative phosphorylation at baseline (n=4) to levels following ILE (n=5).

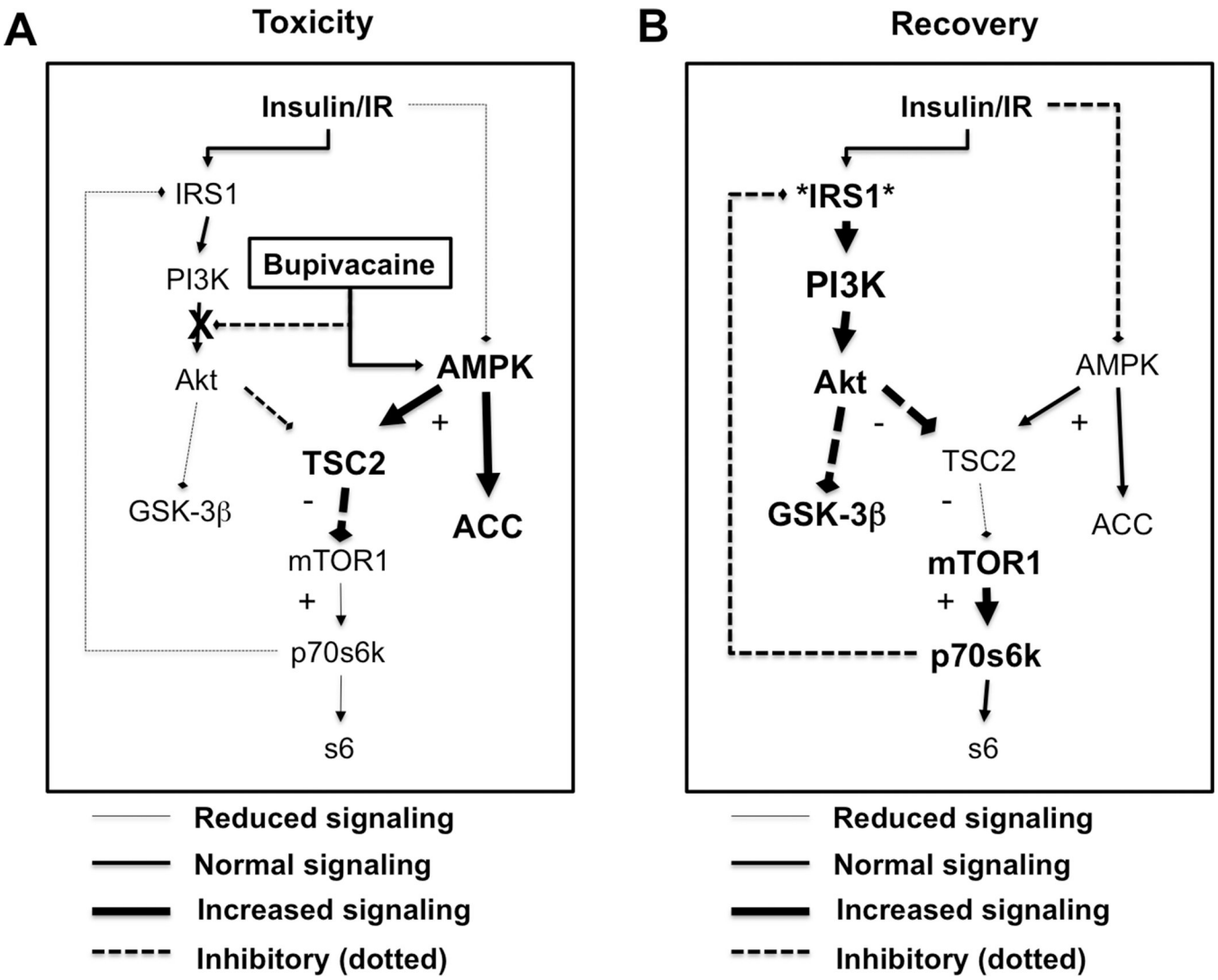

Figure 10. Schematic of induction of and recovery from bupivacaine toxicity

A. During toxicity, bupivacaine activates 5' adenosine monophosphate activated protein kinase (AMPK) with phosphorylation of threonine 172 and blocks protein kinase B (Akt) with reduction of phosphorylation at serine 473 and some reduced phosphorylation of Threonine 308. These two effects converse at tuberous sclerosis 2 (TSC2). AMPK activates TSC2 by phosphorylating it at serine 1387 with a decrease of inhibition of TSC2 by Akt. Kinases downstream of the mammalian target of rapamycin complex 1 (mTOR1) including p70 s6 kinase (p70s6k) and ribosomal protein s6 (s6) will be less activated. Feedback inhibition of insulin receptor substrate 1 (IRS1) by p70s6k is lost leading to sensitization of insulinergic signaling. **B**. During recovery, IRS1 is hyper-sensitized so at equivalent insulinergic stimulation there will be a hyper-activation of kinases downstream of IRS1 including Akt and glycogen synthase kinase 3β (GSK-3β). Both of these proteins can control and assist with recovery of cardiac contractility. AMPK remains phosphorylated and targets downstream of TSC2 and mTOR1 remain un-activated.

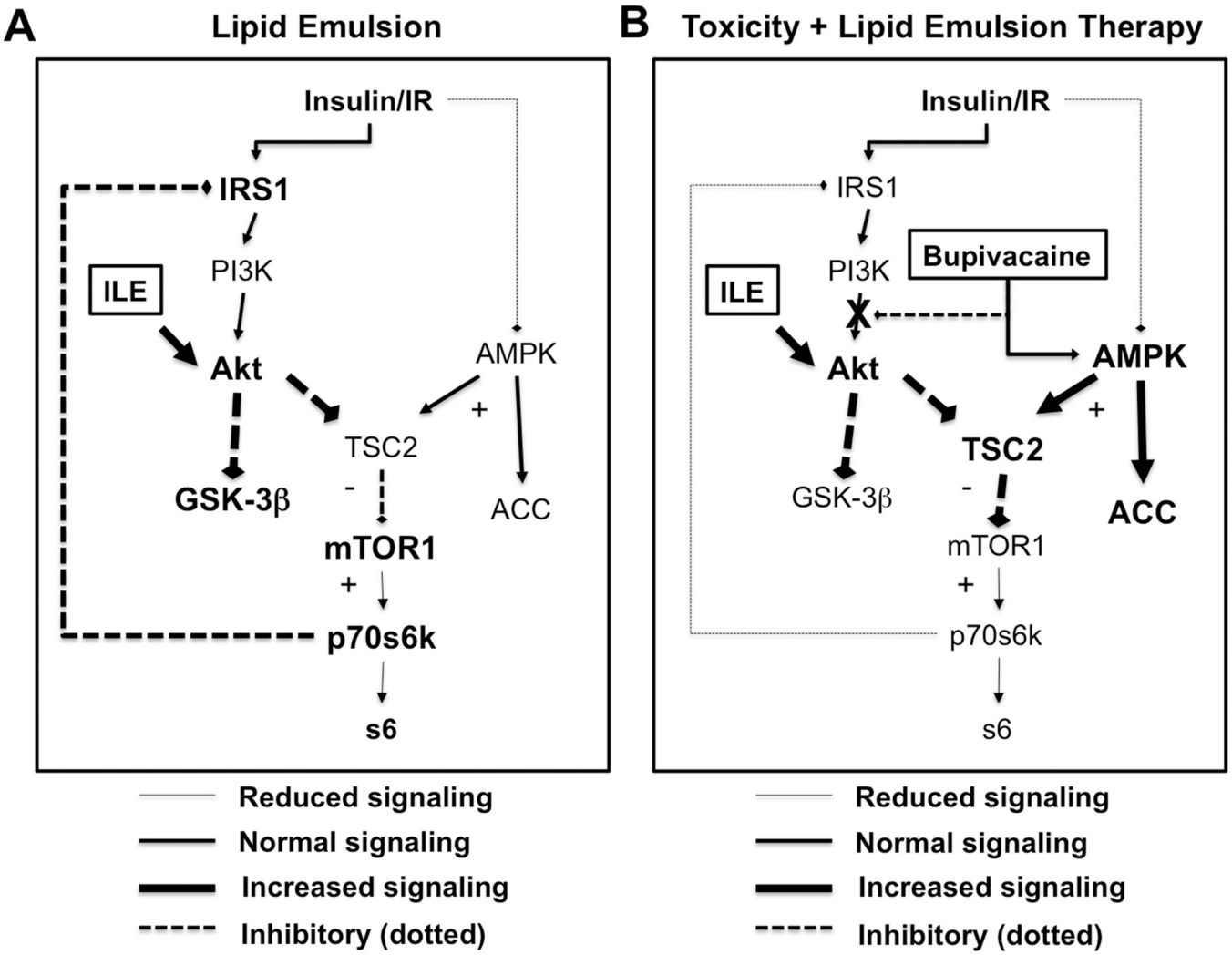

Figure 11. Schematic of contribution of lipid emulsion to treatment of bupivacaine toxicity

A. On its own lipid emulsion (ILE, 10mL/kg Intralipid) rapidly activates insulinergic signaling in cardiac tissue with phosphorylation of protein kinase B (Akt) at both threonine 308 and serine 473. This leads to feedback phosphorylation of insulin receptor substrate (IRS1). ILE had no observable effect on 5' adenosine monophosphate protein activated kinase (AMPK) or downstream targets including acetyl CoA carboxylase (ACC) or tuberous sclerosis 2 (TSC2) and did not contribute to inhibition or activation of mammalian target of rapamycin complex 1 (mTOR1), p70 s6 kinase (p70s6k) or ribosomal protein s6 (s6) **B**. During toxicity, bupivacaine blocks Akt signaling and activate AMPK signaling with blockade of downstream proteins including p70s6k & s6 via inhibition of mTOR1 by TSC2. Adjuvant lipid emulsion will cause phosphorylation of Akt at threonine 308 and serine 473. AMPK signaling remains activate due to bupivacaine toxicity with continued loss of signaling downstream mTOR1. With persistent activation, IRS1 does not immediately re-sensitize.